Article

Voluntary exercise does not always suppress lung cancer progression

LLC1 Lung Cancer Cells
Subcutaneous Injection

LLC1.1 Lung Cancer Cells
B16F10 Melanoma Cells
Intravenous Injection

BLOCKED

No Difference in
Tumor Growth

No Difference in
Colonies Number

2-15 km/day

Reduced Tumor
Growth

>15 km/day

Aurelia C.
Leimbacher,
Philipp Villiger,
Nina Desboeufs,
..., Thomas J.
Haider, Max
Gassmann,
Markus Thiersch

markus.thiersch@uzh.ch

Highlights

Voluntary wheel running
does not suppress lung
cancer in an orthotopic
mouse model

Moderate exercise does
not suppress lung invasion
of B16F10 melanoma cells

Moderate exercise does
not suppress
subcutaneously growing
lung tumors

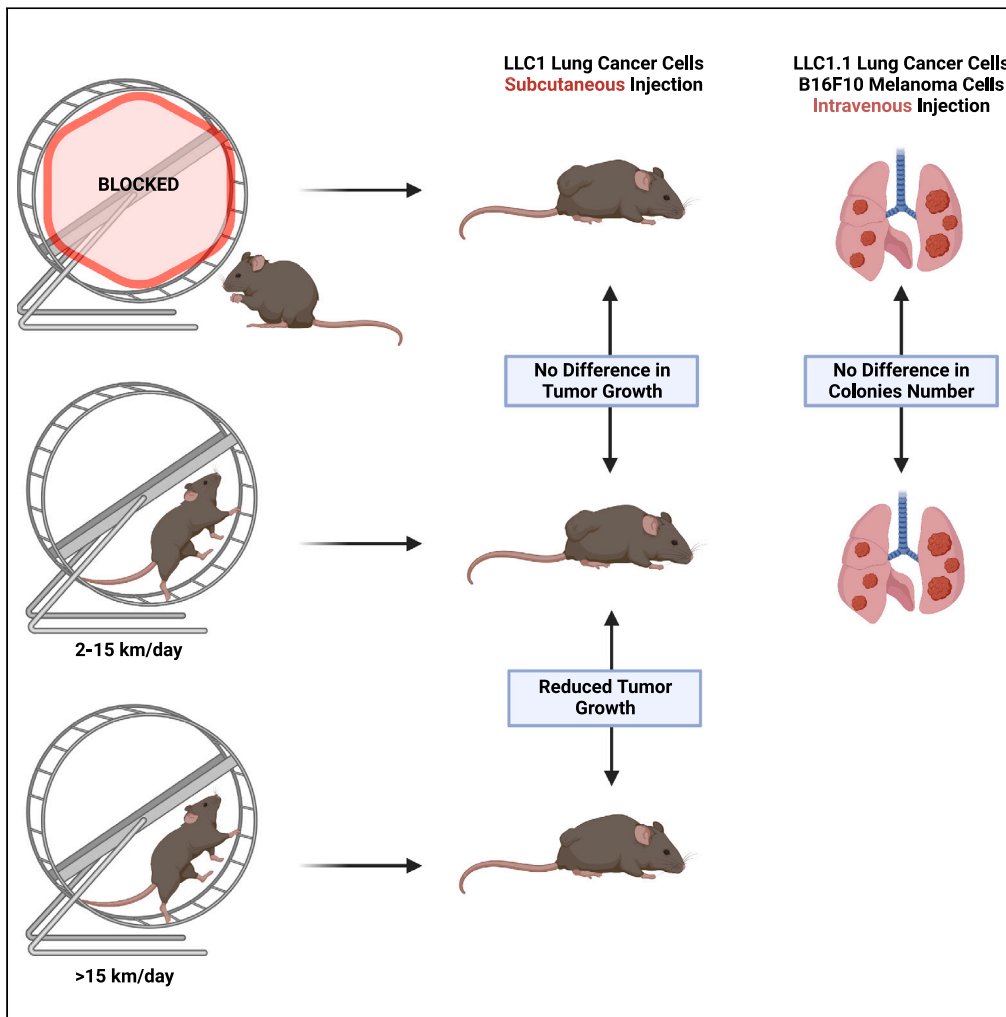High voluntary exercise
may suppress
subcutaneously growing
lung tumors

Article

Voluntary exercise does not always suppress lung cancer progression

Aurelia C. Leimbacher,[1,8] Philipp Villiger,[1,8] Nina Desboeufs,[1,8] Mostafa A. Aboouf,[1,2,3,4] Monica Nanni,[1] Julia Armbruster,[1] Hyrije Ademi,[1] Pascal Flüchter,[5] Maja Ruetten,[6] Felix Gantenbein,[7] Thomas J. Haider,[1] Max Gassmann,[1,2] and Markus Thiersch[1,2,3,9,*]

SUMMARY

Physical exercise can lower lung cancer incidence. However, its effect on lung cancer progression is less understood. Studies on exercising mice have shown decreased ectopic lung cancer growth through the secretion of interleukin-6 from muscles and the recruitment of natural killer (NK) cells to tumors. We asked if exercise suppresses lung cancer in an orthotopic model also. Single-housed C57Bl/6 male mice in cages with running wheels were tail vein-injected with LLC1.1 lung cancer cells, and lung tumor nodules were analyzed. Exercise did not affect lung cancer. Therefore, we also tested the effect of exercise on a subcutaneous LLC1 tumor and a tail vein-injected B16F10 melanoma model. Except for one case of excessive exercise, tumor progression was not influenced. Moderately exercising mice did not increase IL-6 or recruit NK cells to the tumor. Our data suggest that the exercise dose may dictate how efficiently the immune system is stimulated and controls tumor progression.

INTRODUCTION

Physical exercise protects against the development and progression of a broad spectrum of cancer types. It reduces the incidence of at least 13 types of cancer,[1] tumor growth, and metastasis.[2,3] Exercise can enhance drug tolerance and treatment efficacy[4] and inversely correlates with recurrence rates.[5] It can also prevent comorbidities such as cancer cachexia,[6] anemia,[7] or psychological symptoms such as depression or anxiety.[8] Mechanistically, exercise alters the tumor microenvironment by targeting four physiological mechanisms: (1) tumor vascularization and oxygenation, (2) anaerobic cancer metabolism, (3) myokine production in activated muscles, and (4) activation of tumor-suppressing immune cells.[3,9,10] Two or more of these pathways are most likely activated simultaneously during exercise and act in concert to suppress tumor development and growth. For example, the release of lactate from exercising muscles or the release of the stress hormone epinephrine from adrenal glands activates cytotoxic, tumor-suppressive CD8+ cells,[11] or natural killer cells,[12] respectively. Working skeletal muscles release cytokines (myokines)[13] that engage a muscle to cancer crosstalk or activate tumor-suppressive immune cells. Many myokines, such as musclin, irisin, SPARC, interleukin 15, and fibroblast growth factor 21, can directly suppress tumorigenesis, e.g., by targeting the cancer cell's metabolism, suppressing proliferation, preventing metastasis, or inducing apoptosis (reviewed in[14]). Additionally, myokines such as interleukin 15, brain-derived neurotrophic factor, or irisin can indirectly affect tumorigenesis, e.g., by targeting the patient's metabolism and preventing cancer cachexia, fat accumulation-dependent changes in the tumor microenvironment, insulin resistance, or chronic inflammation (reviewed in[14]). Low-intensity exercise slightly upregulates cytokines such as fractalkine (CX3CL1).[15] High-intensity exercise differentially regulates more than 900 genes in muscles and other tissues.[16] It stimulates the expression and release of chemotactic myokines such as CX3CL1 and CCL1[17,18] or monocyte chemotactic protein, interleukin 8, vascular endothelial growth factor, and interleukin 6 (IL-6), etc.[18]

IL-6, the best-studied myokine, is acutely secreted from working muscles,[19] depending on the type, intensity, and duration of exercise,[20] and directly or indirectly suppresses cancer.[14] The IL-6 release peaks at the end of an exercise bout and declines rapidly to pre-exercise levels when the muscles rest.[21–23] Such rapid changes in IL-6 levels are mirrored by rapid changes in immune cell counts in the blood. The number of natural killer (NK) and T-cells in the blood increases within minutes during exercise[24–26] due to the mobilization of preexisting cells from bone marrow and peripheral organs.[11,12,27] After plateauing, these

[1]Institute of Veterinary Physiology, Vetsuisse Faculty, University of Zurich, 8057 Zurich, Switzerland

[2]Zurich Center for Integrative Human Physiology (ZIHP), University of Zurich, 8057 Zurich, Switzerland

[3]Center for Clinical Studies, Vetsuisse Faculty, University of Zurich, 8057 Zurich, Switzerland

[4]Department of Biochemistry, Faculty of Pharmacy, Ain Shams University, Cairo 11566, Egypt

[5]Institute of Physiology, University of Zurich, Zurich, Switzerland

[6]PathoVet AG, Pathology Diagnostic Laboratory, 8317 Tagelswangen ZH, Switzerland

[7]Zurich Integrative Rodent Physiology (ZIRP), University of Zurich, 8057 Zurich, Switzerland

[8]These authors contributed equally

[9]Lead contact

*Correspondence:
markus.thiersch@uzh.ch
https://doi.org/10.1016/j.isci.2023.107298

mobilized cells are redistributed into peripheral organs,[28] resulting in a rapid post-exercise drop of circulating NK or T-cells.[24,29] NK and T-cells activated by exercise can suppress tumor growth and metastasis in various myeloma, mammary carcinoma, melanoma, or lung cancer models.[11,12,30]

However, lung cancer, by far the leading cause of cancer death,[31] is underrepresented in preclinical studies,[2,3] despite the promising effects of exercise in human lung cancer patients. Exercise lowers the lung cancer risk, especially in smokers.[32] In patients with lung cancer, exercise ameliorates fatigue and improves pulmonary function, cardiorespiratory fitness, strength, and quality of life.[33] Whether exercise impacts progression, metastasis, or treatment success in lung cancer patients is less clear. Human serum isolated immediately after exercising reduced the growth of human A549 lung cancer cells by attenuating the AKT/mTOR pathway,[34] suggesting that exercise indeed suppresses lung cancer growth. In mice, anaerobic but not aerobic exercise reduces the incidence of urethan-induced lung tumors.[35] Voluntary exercise in running wheels reduced tumor growth in two lung cancer models using tail vein-injected human A549 cells[36] and subcutaneously injected murine LLC1 cells,[12,37] although another study on LLC1 lung tumors did not report reduced tumor growth in voluntary exercise mice.[38] However, the A549 and LLC1 tumor models have intrinsic limitations. The tail vein injection of A549 cells targets the lung of immunodeficient SCID mice. Still, it neglects the role of the adaptive immune system and, at least partially, the NK cell function in tumor development.[39] The LLC1 mice were injected into immunocompetent mice, however, subcutaneously, without replicating the natural tumor microenvironment that may affect tumor progression and therapeutic response.[40] Therefore, we asked if exercise suppresses tumor growth in an orthotopic lung cancer model. To answer our question, we used LLC1.1 lung cancer cells, which are prone to invade the lung after tail vein injection,[41] and injected them into mice voluntarily exercising in running wheels or not. To test if the results obtained with our orthotopic LLC1.1 model differ from those of previously used ectopic models, we analyzed the effect of voluntary exercise on tumor progression also in a subcutaneously injected LLC1 lung cancer and a tail-vein injected B16F10 melanoma model.

RESULTS

Voluntary exercise in running wheels does not suppress invasion and growth of LLC1.1 lung cancer cells in the lungs of C57Bl/6 mice

C57Bl/6 mice were single-housed in cages with open or blocked running wheels, and the daily running distance was recorded. The daily running distance increased from an average of 2.5 ± 0.7 km per day in the first week (day 1–7) to 5.2 ± 0.6 km per day in the second week (day 8–14) and remained stable around 4.4 ± 0.6 km per day until LLC1.1 cancer cell injection (Figure 1A). After injecting LLC1.1 cells into the tail vein, the daily running distance gradually declined to 1.5 ± 0.9 km per day in the last week before euthanizing the mice. Voluntary exercise in running wheels did not alter the number of tumor nodules visible on the lung surface or the tumor area relative to the total lung area in histological sections (Figures 1B and 1C). Using a Pearson correlation analysis, we observed that the number of metastatic colonies did not correlate with the daily running distance before cancer cell injection (r = −0.6; p = 0.16) or after cancer cell injections (r = 0.019; p = 0.97) (Figure 1D), suggesting that voluntary exercise did not affect lung infiltration and proliferation of LLC1.1 lung cancer cells. The IL-6 levels in plasma isolated during the active (dark phase) from LLC1.1 lung cancer mice were not elevated compared to tumor-free control mice and did not differ between non-running and running mice (Figure 1E). The LLC1.1 lung cancer model develops anemia of cancer (Figure 1F). We observed that voluntary exercise partially recovered anemia by increasing the hematocrit from 31.7 to 35.7% (p = 0.008) and the hemoglobin levels from 10.4 to 11.3 g/dL (p = 0.07) in anemic LLC1.1 tumor mice. To test if partially recovered hematocrit and hemoglobin levels impact tumor hypoxia, we analyzed HIF-2α in lung sections of running and not-running mice with LLC1.1 lung cancer. Voluntary exercise lowered the expression of HIF-2α in lung cancer nodules by a factor of 6.8 (p = 0.004) as well as the HIF-2a expression in the entire lung by a factor of 3.3 (p = 0.052) (Figure 1G) suggesting that voluntary exercise and the associated partial restoration of red blood cells may improve tissue oxygenation in the lung. Despite better lung oxygenation, voluntary exercise did not affect the number of Ki67-positive proliferating cancer cells in tumor nodules of LLC1.1 tumor mice (Figure 1G), further suggesting that voluntary exercise during a 6-week training phase was not sufficient to prevent invasion and proliferation of LLC1.1 cells in the lung.

Voluntary exercise in running wheels does not prevent invasion and growth of B16F10 melanoma cells in the lungs of C57Bl/6 mice

To test if the lack of exercise-induced protection from LLC1.1 lung cancer was model-specific, we used a B16F10 melanoma lung colonization mouse model, which showed tumor suppression after and during
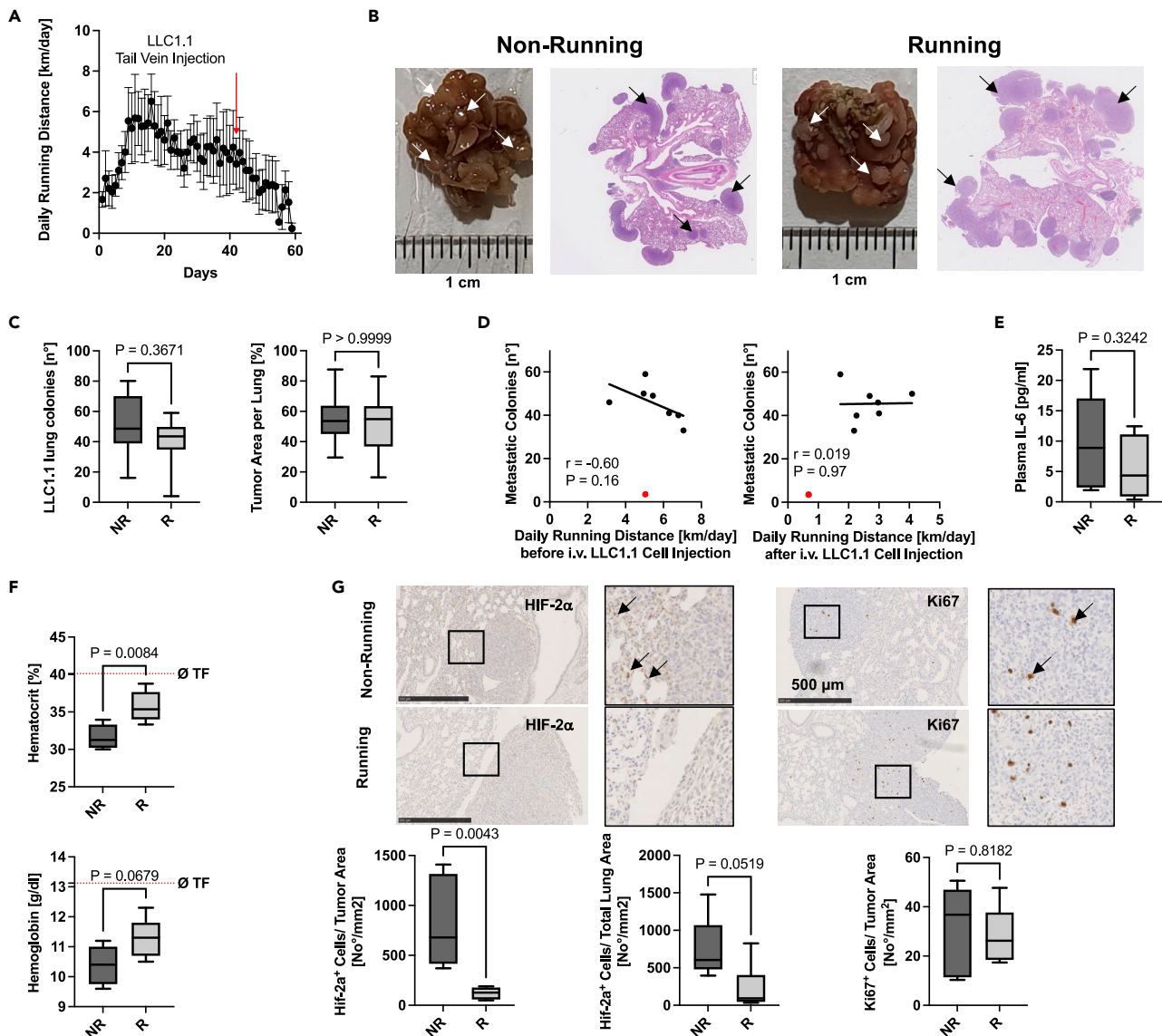
Figure 1. The effect of voluntary exercise in running wheels on LLC1.1 tumor growth in lungs of C57Bl/6 mice

C57Bl/6 male mice were single-housed in cages with an open (running) or blocked running wheel (non-running). After six weeks, LLC1.1 lung cancer cells were tail vein injected (3.3×10^5 cells in 100 μL HBSS). Mice were placed back into their cages. Lungs were isolated 15–17 days after cancer cell injection when body weight dropped by 6%.

(A and B) Shown is the average and standard deviation of the daily running distance of 8 mice kept in cages with an open running wheel before (day 0–44) and after LLC1.1 tail vein injection. Panel B shows representative images of LLC1.1 tumor nodules (left panels) in the lungs of non-running and running mice 15–17 days after the tail vein injection of LLC1.1 cells. The right panels show representative hematoxylin/eosin-stained lung sections of non-running and running mice. Arrows indicate tumor nodules on isolated lungs (white arrows) and hematoxylin/eosin-stained lung sections (black arrows, right).

(C) Shown is the count of LLC1.1 tumor nodules per lung (left panel) and the ratio of tumor to total lung area estimated from hematoxylin/eosin-stained lung section (right panel) of non-running (NR) and running (R) mice 15–17 days after the tail vein injection of LLC1.1 cells (n = 8).

(D–G) Shown is the Pearson correlation analysis of the tumor nodule count (y axis) vs. average daily running distance (x axis) of individual mice before (left panel) and after tail vein injection of LLC1.1 lung cancer cells (right panel). The red data points were excluded as outliers from the analysis. Further shown are E interleukin 6 (IL-6) levels in the blood and F hematocrit (upper panel) and hemoglobin (lower panel) of LLC1.1 tail vein-injected non-running (NR) and running mice (R) 15–17 days after the tail vein injection of LLC1.1 cells (n = 5–6). The red dotted line indicates the average (Ø) value of four tumor-free (TF) mice. Panel G shows representative images of immunohistochemically analyzed lung sections of LLC1.1 tail vein-injected non-running (images upper row) and running (images lower row) mice 15–17 days after the tail vein injection of LLC1.1 cells. The sections were probed for HIF-2α (left panels) and Ki67 (right panels). The black arrows indicate Ki67 and HIF-2α positive cells. Further shown is the quantification of Ki67 and HIF-2α positive lung sections (lower panels) normalized to tumor area (left and middle panel) and normalized to total lung area (right panel) of LLC1.1 tail vein-injected non-running (NR) and running mice (R) (n = 5–6). Data are shown as boxplots with min to max whiskers and were analyzed using a Student's *t* test.

exercise in running wheels.[12] C57Bl/6 mice were single-housed in cages with open or blocked running wheels, and the daily running distance was recorded. The daily running distance increased from an average of 2.9 ± 0.8 km per day in the first week (day 1–7) to 5.9 ± 1.2 km per day in the second week (day 8–14) and remained stable around 7.2 ± 0.4 km per day until B16F10 melanoma cell injection (Figure 2A). After the injection of B16F10 cells, the daily running distance remained constant at 5.2 ± 0.2 km per day. Unexpectedly, voluntary exercise with running wheels did not alter the number of tumor nodules visible on the lung surface (Figure 2B) in two independent experiments (Figure 2C). Using a Pearson correlation analysis, we observed that the daily running distance before cancer cell injection ($r = -0.2$; $p = 0.35$) or after cancer cell injections ($r = -0.55$; $p = 0.3$) did not affect the number of metastatic colonies (Figure 2D). In contrast to a previous study,[12] our data suggest that voluntary exercise before and after B16F10 tail vein injection does not reduce the lung infiltration of B16F10 melanoma cells in male C57Bl/6 mice. The IL-6 levels in plasma isolated during the active (dark phase) from B16F10 injected mice were more than 800 times higher than in tumor-free mice (Figure 2E). We detected no statistically significant difference in IL-6 plasma levels between non-running and running mice (Figure 2E). However, some exercising tumor mice had even lower levels than non-running controls reducing the average IL-6 plasma levels from 2139 in non-running to 1131 pg/mL in running mice ($p = 0.22$). In contrast to the LLC1.1 mouse model, non-running B16F10-injected mice did not develop cancer anemia. We observed no difference in hematocrit between running and non-running mice, but the hemoglobin levels dropped slightly from 12.23 g/dL in non-running mice to 11.23 g/dL in running mice ($p = 0.05$) (Figure 2F). Next, we semi-quantified the immune cell infiltration at the periphery (at the contact region of metastases and lung tissue). We scored immune cell infiltration from 0 to 3[42] with scores 0 and 1 indicating a low-grade inflammation and scores 2 and 3 a high-grade inflammation. We observed that voluntary exercise increased the overall score from 0.82 in non-running to 1.5 in running mice. Mice in cages with blocked running wheels displayed low-grade inflammation. Three out of 8 running mice also showed no or low-grade inflammation. The remaining five displayed high-grade inflammation (score 2), suggesting that immune cell infiltration into B16F10 tumor nodules in the lung is increased by exercise. However, the daily running distance did not correlate with the inflammation grade (r-0.26, $p = 0.54$ and r-0.17, $p = 0.70$ for inflammation grade vs. running distance before and after cancer cell injection). Moreover, our data showed that voluntary exercise did not affect B16F10 lung invasion and proliferation despite the increased immune cell infiltration.

Voluntary exercise in running wheels does not suppress tumor growth of subcutaneously implanted LLC1 lung cancer cells in most C57Bl/6 mice

Next, we tested in four independent experiments if the growth of subcutaneously implanted LLC1 lung cancer cells can be suppressed, as reported before.[12] C57Bl/6 mice were single-housed in cages with open or blocked running wheels, and the daily running distance was recorded. The daily running distance in experiment 1 increased from an average of 2.5 ± 0.9 km per day in the first week (day 1–7) to 6.5 ± 1.4 km per day in the second week (day 8–14) and remained stable around 6.82 ± 0.5 km per day until the subcutaneous LLC1 lung cancer cell injection (Figure 3A). After the LLC1 implantation, the daily running distance decreased to 3.8 ± 0.5 km per day. Similar to tail vein injected LLC1.1 lung cancer cells, the subcutaneous LLC1 model developed anemia of cancer. However, voluntary exercise did not affect hematocrit and hemoglobin levels (Figure S1). Voluntary exercise in running wheels did not alter the tumor weight in two independent experiments (experiments 1 and 3) (Figure 3B). However, in experiment 2, voluntary exercise increased the LLC1 tumor weight from 0.8 g in non-running to 1.1 g in running mice ($p = 0.04$). In experiment 4, voluntary exercise decreased the LLC1 tumor weight from 0.75 g in non-running to 0.42 g in running mice ($p = 0.001$) (Figure 3B). Next, we performed a correlation analysis of tumor weight vs. average daily running distance to analyze why some LLC1 implanted tumor mice responded with a reduced tumor weight to exercise while the tumor weight in most mice was not affected by voluntary exercise (Figure 3C). Tumor weight negatively correlated with the daily running distance before ($r = -0.24$, $p = 0.06$) and after ($r = -0.29$, $p = 0.02$) LLC1 implantation (Figure 3C, **upper panels**) as well as with overall (i.e., before and after LLC1 injection) daily running distance (Figure S2A). These data indicate that increased levels of exercise may reduce the progression of LLC1 tumors. However, this effect resulted mainly from data from experiment 4, where voluntary exercise reduced the tumor weight. These mice showed a much higher daily running distance than mice of experiments 1–3 before (1.6 times) and after (7.3 times) the LLC1 cell injection and throughout the entire experiment (3 times), respectively. While the daily running distance decreased in experiments 1–3 after the LLC1 implantation, the daily running distance of mice in experiment 4 increased after the LLC1 implantation (Figure S2B). When we performed correlation analyses without data from experiment 4, the daily running
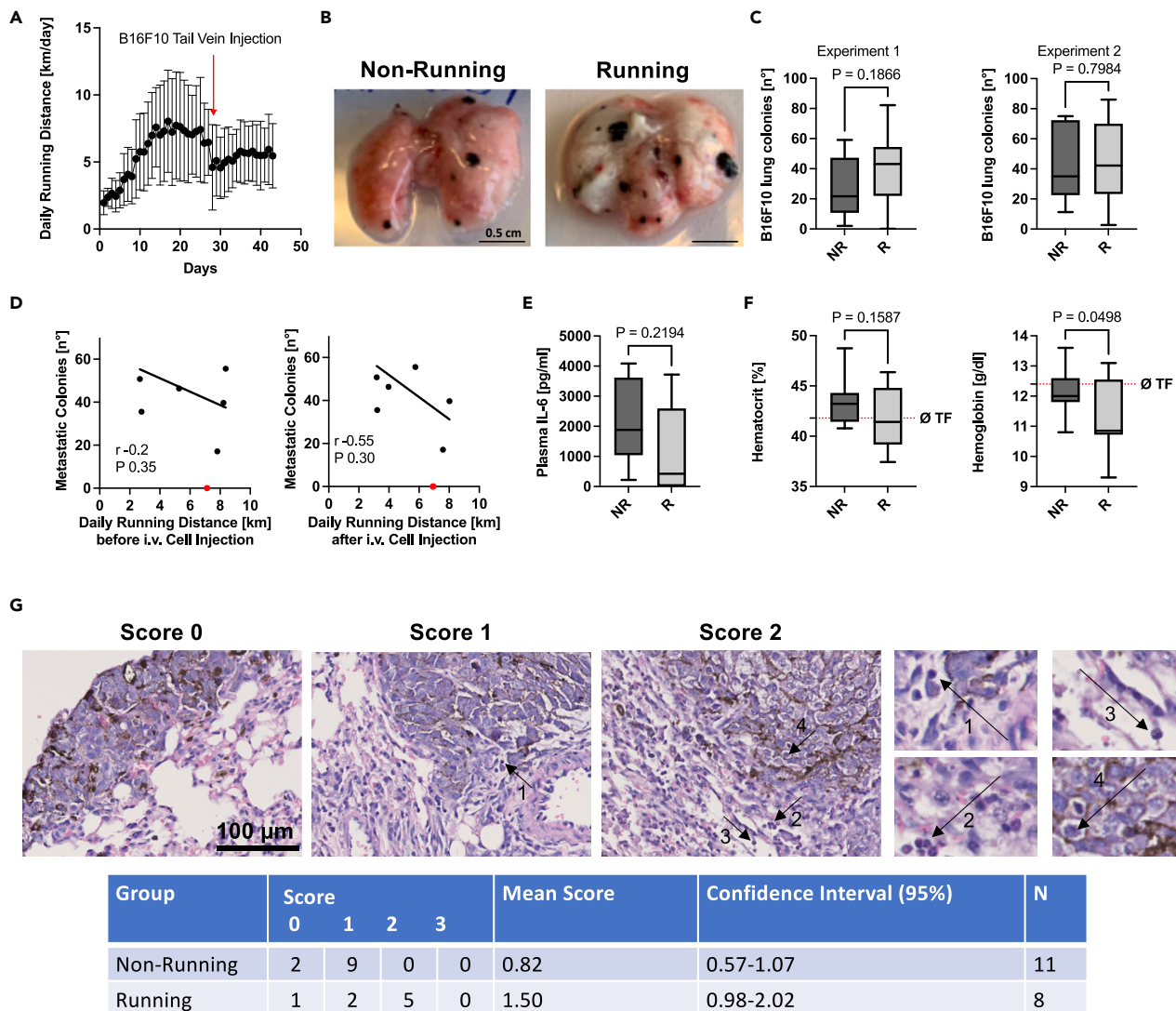
Figure 2. The effect of voluntary exercise in running wheels on B16F10 melanoma growth in lungs of C57Bl/6 mice

C57Bl/6 male mice were single-housed in cages with an open (running) or blocked running wheel (non-running) for four weeks. After four weeks, B16F10 melanoma cells were tail vein injected (2×10^5 cells in 100 μL HBSS). Mice were placed back into their cages with either open or blocked running wheels. Lungs were isolated 16 days after injection. Two independent experiments were performed.

(A and B) Shown is a representative graph (experiment 1) of the average and standard deviation of the daily running distance of 8 mice kept in cages with an open running wheel before (day 0–28) and after the tail vein injection of B16F10 melanoma cells. Panel B shows representative images of black B16F10 tumor nodules in the lungs of non-running (left) and running (right) mice 16 days after the tail vein injection of B16F10 cells.

(C–G) Shown is the count of B16F10 tumor nodules in the lungs of non-running (NR) and running (R) mice from experiment 1 (left panel) and experiment 2 (right panel) 16 days after the tail vein injection of B16F10 cells. Data are shown as boxplots with min to max whiskers and were analyzed using a Student's test. (n = 8–11). Panel D shows the Pearson correlation analysis of tumor nodule count (y axis) vs. average daily running distance (x axis) of individual mice before (left panel) and after (right panel) tail vein injection of B16F10 melanoma cells. The red data points were excluded from the Pearson correlation analysis (outlier). Further shown are E Interleukin (IL-6) levels in the blood and F hematocrit (left panel) and hemoglobin (right panel) of B16F10 tail vein-injected non-running (NR) and running mice (R) (n = 5–6). Data are shown as boxplots with min to max whiskers and were analyzed using a Student's *t* test. The red dotted line indicates the average (Ø) value of four tumor-free (TF) mice. Panel G shows immune cell infiltration into B16F10 tumor nodules in representative hematoxylin/eosin-stained lung sections with score 0 (left panel, no immune cell infiltration), score 1 (middle panel, moderate immune cell infiltration without tissue damage), and score 2 (right panel, immune cell infiltration with tissue damage). The score of immune cell infiltration at the metastasis edges was assessed blinded, and data are shown in the table below (n = 8–11). The arrows indicate lymphocytes (arrow 1), neutrophilic granulocytes (arrow 2), macrophages (arrow 3), and apoptotic cells (arrow 4).
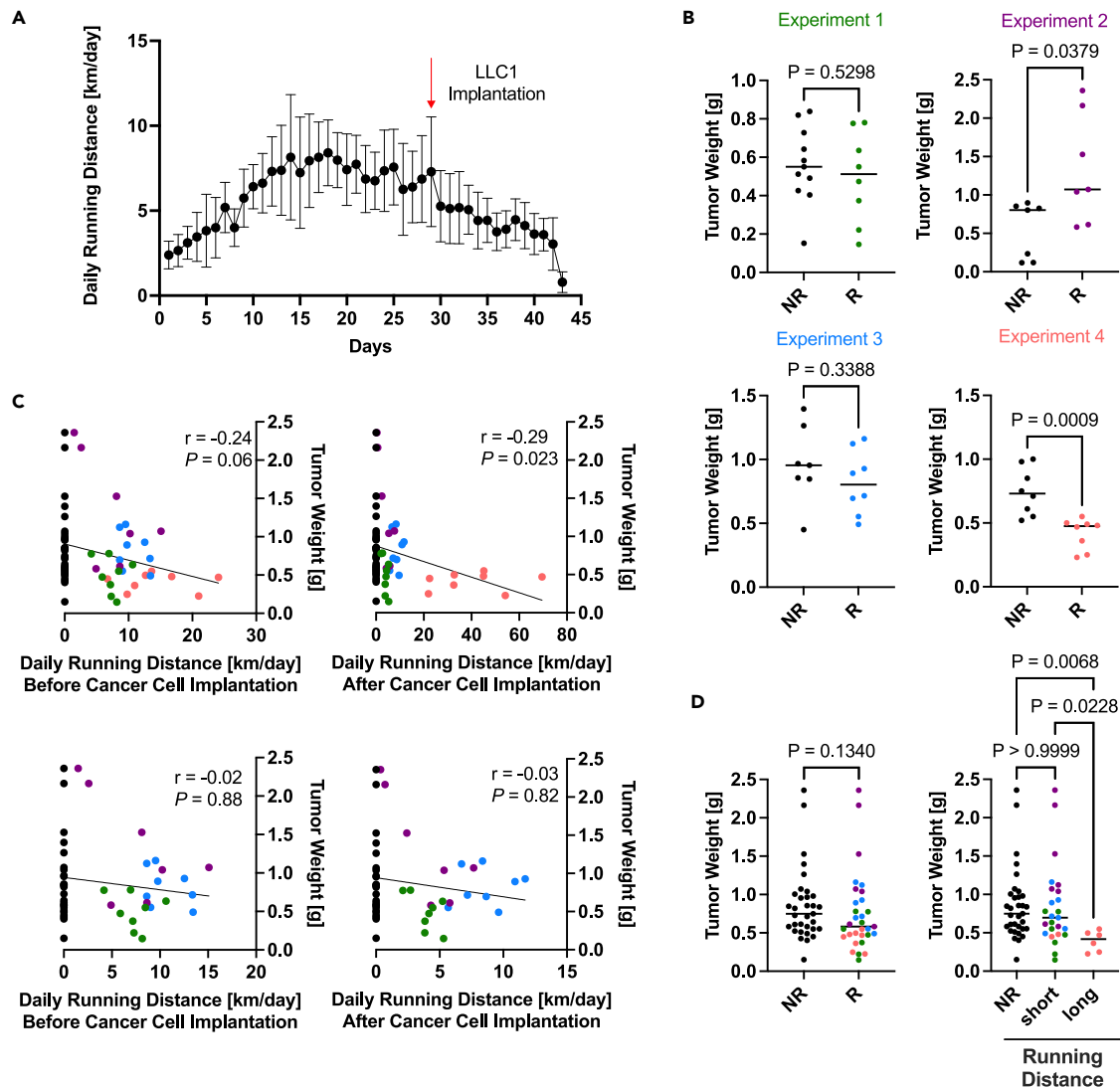
Figure 3. The effect of voluntary exercise in running wheels on subcutaneous LLC1 tumor growth in C57Bl/6 mice

C57Bl/6 male mice were single-housed in cages with an open (running) or blocked running wheel (non-running) for four weeks. After four weeks, LLC1 lung cancer cells were subcutaneously injected (5×10^5 cells in 100 μL HBSS/Matrigel). Mice were placed back into their cages with either open or blocked running wheels. Tumors were isolated and weighed 21 days after implantation. The experiment was repeated independently three times (experiments 1–4).

(A) Shown is a representative graph (experiment 1) of the average and standard deviation of the daily running distance of 8 mice kept in cages with an open running wheel before (day 0–30) and after LLC1 implantation (day 31–48).

(B) Shown is the tumor weight of non-running (NR) and running (R) mice 21 days post LLC1 cancer cell implantation. Data are shown as a scatter dot blot and median indicating the tumor weight of individual non-running mice (black circles in all panels) and running mice from the first (green circles, upper left panel), second (purple circles, upper right panel), third (blue circles, lower left panel), and fourth (red circles, lower right panel) independent experiment (n = 7–10). A Student's *t* test or a Mann-Whitney test (Experiment 2) was performed.

(C) Shown is the Spearman correlation analysis of tumor weight (y axis) vs. the average daily running distance (x axis) before (left panels) or after (right panels) tumor cell injections of individual mice from the first (purple), second (green), and third (blue) experiment with (upper panels, n = 64) and without (lower panels, n = 48) data of the 4th experiment (red). The black data points indicate the tumor weight of individual non-running mice at x = 0.

(D) The left panel shows the overall tumor weight comparison of non-running (NR) and running (R) mice from the four independent experiments (first (green), second (purple), third (blue), and fourth (red)) (n = 32–35). The right panel shows the tumor weight of non-running (NR), short-distance (average daily running distance <15 km/day), and long-distance (average daily running distance >15 km/day) running mice (n = 7–35). A Student's *t* test or a one-way ANOVA with Bonferroni post hoc test was performed.

distance correlated with tumor weight, neither before nor after LLC1 cell implantation (Figure 3C lower panels and Figure S2A). However, the largest tumors grew in mice with the lowest daily running distance (purple data points). Finally, we compared the LLC1 tumor weight of non-running and running mice, including data from all 4 experiments. The average tumor weight did not differ between non-running and running mice, suggesting that exercise did not affect tumor progression (Figure 3D). However, when we stratified mice with very long daily running distances (>15 km/day) from mice with moderate running distances (<15 km/day), we observed the tumor weight in mice running long distances was 54.1% (p = 0.007) and 52.8% (p = 0.02) lower than in non-running and moderately running mice, respectively. A difference between non-running and moderately running mice was not observed, suggesting that high exercise levels may be required to suppress tumor growth.

Moderate voluntary exercise in running wheels does not increase muscle-derived interleukin 6 levels in C57Bl/6 mice with subcutaneously implanted LLC1 lung cancer cells

Muscle-derived IL-6 has been reported to be involved in exercise-induced LLC1 tumor suppression.[12] To determine why moderate voluntary exercise (average daily running distance <15 km/day) did not suppress tumor progression in our models, we analyzed plasma IL-6 levels in moderately exercising LLC1 tumor mice (Ø running distance 7.3 $\pm$ 1.9 km/day). Blood was isolated during the night (dark phase) when the running activity of mice was highest. The IL-6 plasma levels were 100 times higher in LLC1 tumor mice than in tumor-free control mice, but we observed no difference between non-running and running LLC1 tumor-bearing mice (Figure 4A). Next, we analyzed IL-6 mRNA expression in muscle, which has been reported to be induced during exercise.[13,23] We observed no difference in *Il-6* mRNA expression in quadriceps and gastrocnemius of non-running and running LLC1 tumor mice, although IL-6 mRNA levels in the gastrocnemius of running mice tended to be slightly higher than in non-running mice (p = 0.11). However, tumor-bearing non-running and running mice seemed to have somewhat lower IL-6 mRNA levels in muscles, especially gastrocnemius, than non-running tumor-free mice (Figure 4B). Correlation analyses showed that neither plasma IL-6 levels nor IL-6 mRNA expression in muscles correlated with average daily running distance (Figure 4C). Because mice ran less when tumor size increased (Figures 3A and S2B), we tested if the average daily running distance at late tumor stages correlated better with IL-6 plasma and muscle mRNA levels. However, we observed no correlation between the average running distance 5 days before tissue isolation (i.e., days 17–21 after LLC1 implantation) and IL-6 plasma or muscle mRNA levels (Figure S3A). The IL-6 mRNA levels in LLC1 tumors of running mice were 40% lower than in non-running mice (p = 0.05) and did not correlate with the average daily running distance (Figures 4D and S3B). IL-6 mRNA levels in the liver were 1.9 times higher in non-running LLC1 tumor mice (p = 0.12) and 2.5 times higher in running LLC1 tumor mice (p = 0.03) than in non-running tumor-free mice. We argue that the increased IL-6 plasma levels in non-running and running mice with LLC1 tumors resulted most likely from tumor and liver IL-6 production, which may have had superimposed exercise-induced IL-6 secretion from muscles in running mice.

Moderate voluntary exercise in running wheels does not recruit natural killer cells to subcutaneously implanted LLC1 tumors in C57Bl/6 mice

Next, we tested if IL-6 production in the liver and tumor in LLC1 tumor mice superimposed muscle-derived IL-6 signaling and affected the previously reported NK cell recruitment into tumors. As previously reported,[12] tumors of running mice showed higher expression of inflammation markers than tumors of non-running mice (Figure 5A). *Il-1b*, *IL-3*, *IL-17a*, and *Tgfb* mRNA levels increased 1.8 times (p = 0.02), 4.1 times (p = 0.06), 2.8 times (p = 0.08), and 1.5 times (p = 0.06), respectively. In contrast, tumor mRNA levels of *Tnfa*, *Infg*, and *iNos* did not differ between running and non-running mice. Genes expression of markers for NK cells, macrophages, and T-cells were not differentially regulated in tumors of running mice (Figure 5A). Immunofluorescence and immunohistochemistry with two different antibodies against NK1.1, which successfully detected NK cells in the spleen, confirmed the absence of NK cells in LLC1 tumors on non-running and running mice (Figure 5B). Additionally, we analyzed circulating immune cells in the blood of non-running and running LLC1 tumor mice by FACS. The proportion of B cells, NK cells, and total CD3⁻ cells did not differ between non-running and running mice (Figure 5C). We further analyzed subpopulations of CD11b/CD27 positive or negative NK cells, which indicate four different NK cell maturation stages from immature (stage 1) to mature (stage 4) in mice[43] and different functions in human NK cells[44] (Figure 5D). The proportion of circulating immature CD11b⁻/CD27⁻ and cytokine-producing CD11b⁺/CD27⁺ NK cells did not differ between non-running and running LLC1 tumor-bearing mice. The ratio of cytokine-producing CD11b⁻/CD24⁺ NK cells increased from 13.5% in non-running
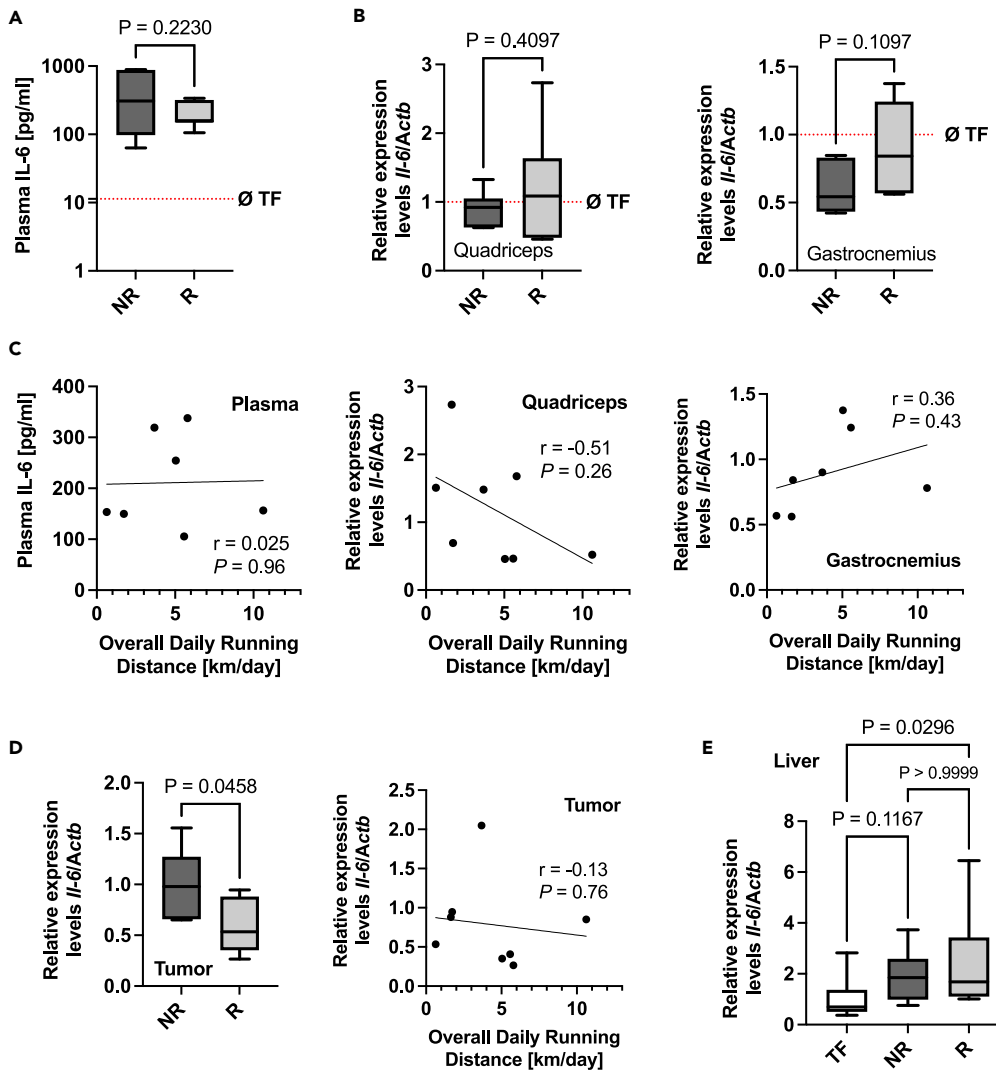
Figure 4. The effect of voluntary exercise in running wheels on muscle-derived interleukin 6 in subcutaneous LLC1 tumor-bearing C57Bl/6 mice

C57Bl/6 male mice were single-housed in cages with an open (running) or blocked running wheel (non-running) for four weeks. After four weeks, LLC1 lung cancer cells were subcutaneously injected (5 x 10^5 cells in 100 μL HBSS/Matrigel). Mice were placed back into their cages. 21 days after implantation, tumors, quadriceps, gastrocnemius, and blood plasma were isolated during high exercise activity at night (dark phase).

(A) Shown are interleukin (IL-6) levels in the blood plasma of non-running (NR) and running mice (R) 21 days after the subcutaneous LLC1 cell implantation (n = 7–8).

(B) Shown are mRNA levels of interleukin 6 (*Il-6*) in quadriceps (left panel) and gastrocnemius (right panel) of non-running (NR) and running mice (R) 21 days after the subcutaneous LLC1 cell implantation quantified by qPCR and normalized to β-actin (*Actb*) mRNA expression levels (n = 5–8).

(C) Shown are Pearson correlation analyses of IL-6 plasma levels (left panel) and *Il-6* mRNA expression levels in quadriceps (middle panel) and gastrocnemius (right panel) vs. average daily running distance (x axis) of individual mice.

(D) The left panel shows mRNA levels of *Il-6* in tumors of non-running (NR) and running mice (R) 21 days after the subcutaneous LLC1 cell implantation quantified by qPCR and normalized to *Actb* mRNA expression levels (n = 6–8). The right panel shows a Pearson correlation analysis of *Il-6* mRNA expression levels in tumors (y axis) vs. average daily running distance (x axis) of individual mice.

(E) Shown are *Il-6* mRNA levels in the liver of tumor-free (TF), non-running (NR), and running mice (R) 21 days after the subcutaneous LLC1 cell implantation quantified by qPCR and normalized to *Actb* mRNA expression levels (n = 7–8). Data are shown as boxplots with min to max whiskers and were analyzed using a Student's *t* test, a Mann-Whitney test, or a Kruskal Wallis test with Dunn's multiple comparison tests (panel E). Ø TF and the red dotted line indicate the average (Ø) value of tumor-free (TF) mice (n = 5–8).
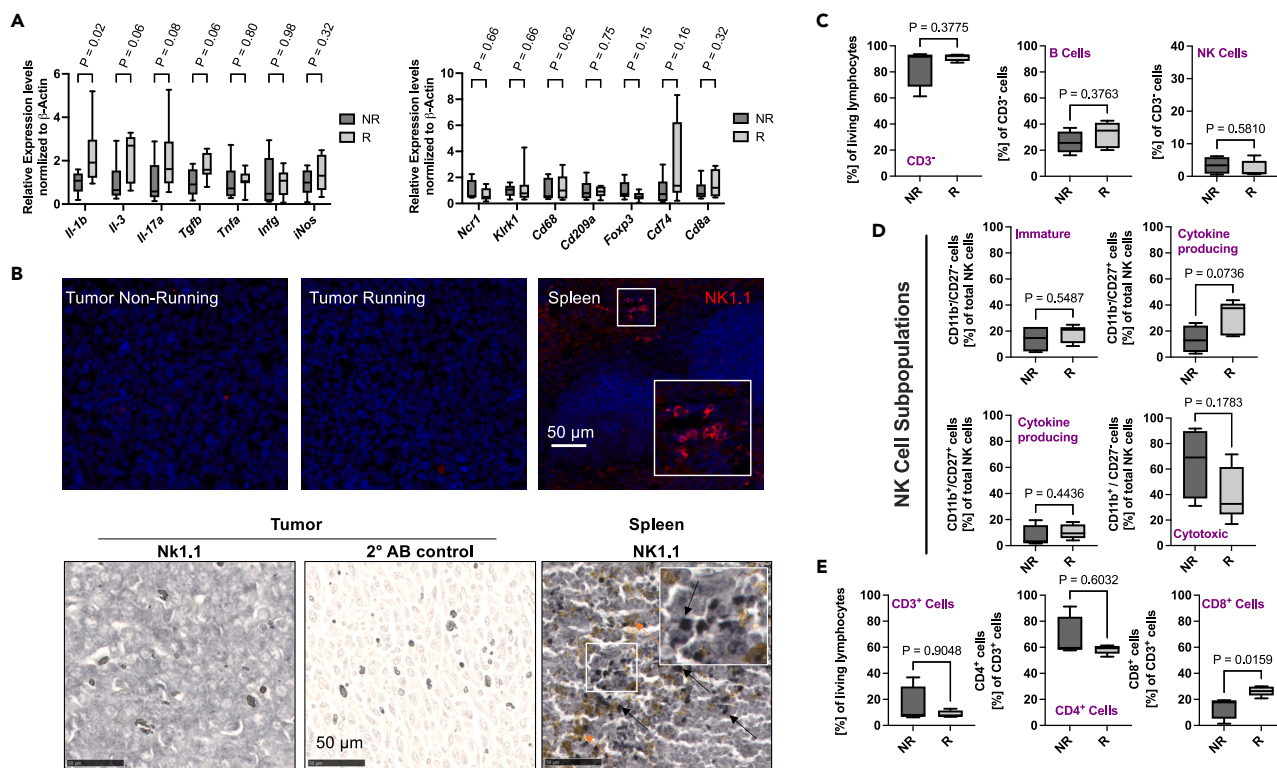
Figure 5. The effect of voluntary exercise in running wheels on the immune cell response in subcutaneous LLC1 tumor-bearing C57Bl/6 mice

C57Bl/6 male mice were single-housed in cages with an open (running) or blocked running wheel (non-running) for four weeks. After four weeks, LLC1 lung cancer cells were subcutaneously injected (5×10^5 cells in 100 µL PBS/Matrigel). Mice were placed back into their cages. 21 days after implantation, blood and tumors were isolated. Immune cells in the blood were analyzed by flow cytometry and in the tumors by immunofluorescence and immunohistochemistry, respectively. Tumor inflammation was analyzed by qPCR.

(A–D) Shown are interleukin 1b (*Il-1b*), interleukin 3 (*Il-3*), interleukin 17a (*Il-17a*), transforming growth factor β (*Tgfb*), tumor necrosis factor alpha (*Tnfa*), interferon-gamma (*Infg*), and inducible nitric oxide synthase (*iNos*) mRNA levels (upper panel) and natural cytotoxicity triggering receptor 1(*Ncr1*) NKp46, killer cell lectin-like receptor subfamily K (*Klrk1*) NKG2-D, CD68 antigen (*Cd68*), CD209 antigen (*Cd209a*), forkhead box P3 (*Foxp3*), CD74 antigen (*Cd74*), and CD8 antigen, alpha chain (*Cd8a*) mRNA levels (lower panel) in LLC1 tumors of non-running (NR) and running mice (R) 21 days after the subcutaneous LLC1 cell implantation quantified by qPCR and normalized to β-actin (*Actb*) mRNA expression levels (n = 6–8). Panel B shows representative images of tumor and spleen paraffin sections of non-running (NR) and running (R) LLC1 tumor-bearing cells analyzed by immunofluorescence (upper panels) and immunohistochemistry (lower panels) for the presence of NK cells. The upper panels show immunofluorescence signals specific for NK1.1 (red) in tumors of non-running (left panel) and running (middle panel) LLC1 tumor-bearing mice as well as in the spleen (positive control) of tumor-free mice (right panel) using the MA1-70100 NK1.1 antibody (Thermo Fisher, Switzerland). DAPI (blue) was used to counterstain the tissue sections. The lower panels show immunohistochemical signals specific for NK1.1 using the BS-4682R NK1.1 antibody (BIOSS, US) in tumors of running LLC1 tumor-bearing mice with (left panel) and without the primary NK1.1 antibody (middle panel, negative control) as well as in the spleen of tumor-free mice (right panel, positive control). The brown signal (orange arrows) in the right panel indicates hemosiderin deposits. Panel C shows the proportion of CD3$^-$ lymphocytes (left panel), B cells (middle panel), and NK cells (right panel) in the blood of non-running (NR) and running (R) mice analyzed by flow cytometry 21 days after the subcutaneous LLC1 cancer cell implantation (n = 4–5). Panel D shows the proportion of subpopulations of NK cells with differential CD27 and CD11b expression, indicating the NK maturation stages[43] and functions[44] in non-running (NR) and running (R) LLC1 tumor-bearing mice analyzed by flow cytometry. Shown are CD27$^-$/CD11b$^-$ cells (left upper panel), CD27$^+$/CD11b$^-$ cells (right upper panel), CD27$^+$/CD11b$^+$ cells (left lower panel3), and CD27$^-$/CD11b$^+$ cells (right lower panel) in the blood of non-running (NR) and running (R) LLC1 tumor-bearing mice (n = 4–5).

(E) Shown is the proportion of CD3$^+$ cells (left panel), CD4$^+$ cells (middle panel), and CD8$^+$ cells (right panel) in the blood of non-running (NR) and running (R) LLC1 tumor-bearing mice analyzed by FACS 21 days after the subcutaneous LLC1 injection (n = 4–5). Data are shown as boxplots with min to max whiskers and were analyzed using a Student's *t* test or a Mann-Whitney test.

---

to 30.6% in running LLC1 tumor mice (p = 0.074). Because the total circulating NK cell proportion did not change (Figure 5C), the increase in CD11b$^-$/CD24$^+$ NK cells may have been at the expense of cytotoxic CD11b$^+$/Cd27$^-$ NK cells, which tended to be lower in running than in non-running mice (Figure 5D). In contrast to NK cells, we observed that the proportion of circulating CD8$^+$ cytotoxic T-cells cells increased from 17.7% in non-running to 26.4% in running LLC1 tumor mice (p = 0.016), while CD4$^+$ and total CD3$^+$ cells did not differ between non-running and running mice (Figure 5E).

DISCUSSION

We investigated if voluntary exercise in running wheels suppresses the tumor progression in an orthotopic LLC1.1 lung cancer mouse model.[41] Running improved oxygenation of lungs and tumor nodules, potentially by reducing anemia of cancer, but did neither affect lung invasion nor proliferation of LLC1.1 cancer cells. Thus, we tested if the lack of exercise-dependent tumor suppression was specific to our orthotopic LLC1.1 model. To validate our data, we tested the effect of exercise in two tumor models in which voluntary running was shown to suppress tumor progression, the B16F10 lung invasion and the subcutaneously injected LLC1 lung cancer model.[12,37] In contrast to these previous studies, we observed that lung invasion in the B16F10 model was not suppressed in running mice in two independent experiments. However, the tumor nodules of running mice showed more immune cell infiltration than those of non-running mice. Similarly, subcutaneous LLC1 tumor growth was not suppressed by voluntary exercise in mice running less than 15 km per day. We found no evidence of muscle-specific IL-6 production in all models tested at late tumor stages. However, high IL-6 plasma levels produced by the liver and tumor may have superimposed muscle-derived IL-6 levels. We observed that voluntary running did not promote the recruitment of NK cells into subcutaneous LLC1 tumors. In the blood, NK cells were not differentially regulated except for an NK subpopulation of cytokine-producing $CD11b^-/CD27^+$ cells, which were upregulated in running mice with LLC1 tumors. In contrast, running increased the levels of cytotoxic $CD8^+$ cells in the blood without detectable consequences for tumor growth. In three different models, voluntary exercise with running wheels did not suppress lung tumor growth and invasion. However, excessive running (i.e., distances longer than 15 km) reduced the weight of subcutaneous LLC1 tumors by 50%. Thus, a higher exercise load, which most mice did not reach, may be required to activate tumor-suppressing mechanisms in the models used in this study.

Most mice, even in the wild, enthusiastically exercise in running wheels.[45] However, the daily running distance and, thus, the performance differs between strains and gender[46] and in-between homogeneous groups. For example, in our study, the most active C57Bl/6 mouse ran 24.1 km/day before cancer cell injection. In comparison, the least active mouse ran 2.6 km/day, confirming the high variability of the exercise volume of voluntarily running mice. We observed that the size of subcutaneous LLC1 tumors in mice running less than 15 km/day was not different from non-running mice. Mice running more than 15 km/day developed smaller LLC1 tumors. Thus, higher exercise volumes, especially before tumor cell implantation,[47,48] may be required to activate tumor suppressive mechanisms in a dose-dependent manner.[49] However, the group of mice running more than 15 km/day in our study exceeded the previously recorded running distances of C57Bl/6 mice. Most mice run between 1.6 and 12.7 km/day,[50] and a few run up to 20 km/day.[49] Some of our mice ran more than 60 km/day. Thus, our data need to be carefully interpreted. Excessive running could result from non-drug addiction to exercise[51,52] or a stress response, such as single-housing, which can even impact tumor incidence and progression.[53,54] Therefore, it is unclear if the reduced tumor size results from voluntary wheel running *per se*. Correlation analyses of mice running less than 15 km/day showed no association between running distance and tumor size. The same was true for the moderately exercising B16F10 and LLC1.1 lung invasion models, suggesting a dose-dependent threshold for exercise to affect tumor progression. Moreover, varying running distances alone cannot explain the discrepancy in subcutaneous LLC1 tumor growth and B16F10 lung invasion between our study and previous studies,[12,37] where the average running distance of mice was similar to or even lower than in our study.[3] However, the authors tested female mice in groups with access to multiple running wheels.[12,37] Group housing prevents isolation stress but may not allow precise and individual recording of running distances. Furthermore, hierarchical structures, existing in groups of male mice and to a lesser extent in groups of female mice, too,[55,56] may prevent the voluntary running of subordinate female mice. Nevertheless, group-housed, running female mice showed consistent tumor suppression,[12,37] indicating that voluntary exercising was insufficient to protect male mice in our and previous studies[38,57] but sufficient to protect female mice against subcutaneous LLC1 tumor growth and B16F10 lung invasion.

In these female mice, the exercise-induced release of IL-6 from muscles reduced tumor growth by recruiting NK cells to the tumor.[12] Muscle-specific IL-6 production increases acutely during exercise and quickly returns to normal levels after exercise.[20,58] However, gender can influence immune responses,[59–61] and it may be possible that exercise induces a sufficiently strong immune response for tumor suppression in C57Bl/6 females but not in males. We isolated plasma and tissues during the dark phase when mice were most active to test this assumption. However, exercise-induced IL-6 declines rapidly after exercise,[23] and we could not control if mice were voluntarily running before isolating the tissues. We observed neither altered IL-6 mRNA expression in muscle, liver, and tumor nor IL-6 plasma levels between running and non-running male mice with LLC1 tumors or B16F10

metastases. However, tumor-bearing mice already had 50-100 times higher IL-6 plasma levels than tumor-free mice, suggesting that the tumor triggered a systemic inflammatory response,[62,63] which may have masked exercise-induced spikes in IL-6 production. Additionally, regular exercise can lead to a training adaptation effect, and plasma IL-6 levels may peak less strongly.[64] Nevertheless, a different IL-6 response between male mice in our study and female mice[12] can explain the absence of NK cells in the LLC1 tumor tissues of our study. Exercising mice showed higher interleukin 1b and 3 mRNA levels in LLC1 tumors than non-running mice. However, the mRNA levels for NK cell, macrophage, and T cell markers did not differ between LLC1 tumors of running and non-running mice. We observed no exercise-induced accumulation of NK cells in tissue sections of subcutaneous LLC1 tumors. Furthermore, we observed only minor changes among the populations of different NK maturation stages in the collected blood samples, although increases of, especially mature, NK cells have been reported during exercise.[12,30,65] Other exercise-induced myokines, such as interleukin 15, or metabolites, such as lactate, can mobilize T-cells.[66,67] Indeed, we observed an increased proportion of CD8$^+$ cells in the blood, which can be metabolically reprogrammed by exercise to reduce tumor growth.[11] We also observed a higher immune cell infiltration into B16F10 lung colonies. However, neither increased CD8$^+$ cells in the blood nor higher immune cell infiltration in B16F10 lung colonies influenced tumor progression.

Despite the lack of tumor suppression, exercise protected the orthotopic LLC1.1 lung cancer mouse model against anemia of cancer, a frequent comorbidity in cancer patients,[68] and reduced hypoxia in lung and tumor tissue. Exercising mice with subcutaneous LLC1 tumors were also reported to be less anemic than their non-exercising controls due to decreased interleukin 1b and lactate levels.[69] However, in our study, exercise did not prevent anemia in mice with subcutaneous LLC1 tumors. Mice with subcutaneous LLC1 tumors but not the orthotopic LLC1.1 model showed increased plasma levels of IL-6, which is also induced in many cancer patients. Although exercise may reduce interleukin 1b and lactate levels to ameliorate anemia,[69] high IL-6 plasma levels can cause functional iron deficiency anemia[70,71] or directly suppress erythropoiesis.[72–74] We assume that strong cancer-associated inflammation and high IL-6 levels can overwrite the beneficial effect of exercise, e.g., by sequestering iron and preventing erythropoiesis. However, in some cases (e.g., with minor inflammation and IL-6 induction), exercise may be beneficial to protect against anemia of cancer.[7]

Limitations of the study

1. Using running wheels for voluntary physical exercise in mice has advantages and disadvantages. Voluntary wheel running is less stressful than forced exercise on a treadmill, does not interfere with the circadian rhythm of mice, and resembles the natural activity pattern of mice.[46] The limitation is, however, the lacking control over exercise volume and intensity. Mice, even inbred siblings, can substantially differ in their running preferences. The varying exercise performances and the resulting heterogeneity in exercise volumes may impact, e.g., tumor progression *per se* or levels of exercise-induced cytokines.

2. Our experimental setup did not allow the precise determination of the running speed, i.e., the exercise intensity. We observed that the daily running distance dropped in most mice with increasing tumor burden. Likewise, tumor burden may have affected exercise intensity which, in turn, may have affected the cancer progression. For example, high-intensity interval training can increase the number of NK cells in obese mammary carcinoma mice[75] and reduce the growth of murine 4T1 mammary tumors.[76] The serum from high-intensity endurance cyclists reduces breast cancer proliferation.[77] In contrast, moderate-intensity endurance training lowered the incidence of liver cancer[78,79] more efficiently than high-intensity interval training.[78] In urethan-induced lung cancer mice, high-intensity interval training and constant moderate-intensity training were reported to reduce tumor growth; however, moderate-intensity training was more efficient than high-intensity training.[80,81] In contrast, another study reported that anaerobic, not aerobic, training prevented urethan-induced lung cancer,[35] and high-intensity interval training on treadmills reduced the growth of subcutaneous LLC1 tumors.[82] Therefore, we cannot rule out whether exercise intensity affected late-stage LLC1 tumor progression in our study.

3. Single housing, required to record individual running performance, is an animal welfare concern. Social species, including mice, experience isolation stress. Because female mice are more prone to isolation stress than male mice, we limited our study to single-housed male C57Bl/6 mice. However, comparing the results of our study to those of studies in female mice[12,37] suggests a gender difference in exercise-dependent protection against cancer in murine LLC1 and B16F10 cancer models. Other group-housing compatible exercise methods may be better suited to test the gender-specific effects of exercise on cancer.

Conclusion

Voluntary wheel running did not protect against cancer in our orthotopic LLC1.1 lung cancer mouse model. Likewise, exercising mice with subcutaneously implanted LLC1 and intravenously injected B16F10 cells were not protected against cancer by voluntary wheel running, despite previous studies (in female mice) reporting up to 50% reduced tumor growth in both models. This inconsistency may be due to the insufficient release of exercise-induced cytokines, such as IL-6, from the muscles of exercising mice into the bloodstream. However, stratifying the mice with subcutaneous LLC1 tumors by their daily running distance revealed reduced LLC1 tumor growth in excessively running mice. This suggests that the exercise dose may dictate if exercise protects against cancer, at least in the subcutaneous LLC1 cancer mouse model. To test how exercise training with defined volume and intensity affects lung cancer, forced exercise training on moto-controlled treadmills for mice using standardized training protocols may help to investigate the dose-dependence of lung cancer suppression by exercise.

STAR★METHODS

Detailed methods are provided in the online version of this paper and include the following:

- KEY RESOURCES TABLE
- RESOURCE AVAILABILITY
  - Lead contact
  - Materials availability
  - Data and code availability
- EXPERIMENTAL MODEL DETAILS
  - Cancer cell lines and cell culture
  - Mice
- METHOD DETAILS
  - Experimental design
  - Histology and immunostainings
  - Quantification of tumor nodules in lungs and immune cell infiltration scoring
  - Plasma Il-6
  - Flow cytometry
  - RNA extraction and mRNA expression analyses
- QUANTIFICATION AND STATISTICAL ANALYSIS

SUPPLEMENTAL INFORMATION

Supplemental information can be found online at https://doi.org/10.1016/j.isci.2023.107298.

AUTHOR CONTRIBUTIONS

Conceptualization, T.H., M.G., and M.T.; Methodology, A.C.L., P.V., N.D., T.H., and M.T.; Validation, P.V., M.A.A., M.N., J.A., P.F., and F.G.; Formal Analysis, A.C.L, P.V., N.D., M.A.A., H.A., M.R., and M.T.; Investigation, A.C.L., P.V., N.D., M.A.A., M.N., J.A., H.A., P.F., F.G., T.H., and M.T.; Resources, M.G., and M.T.; Data Curation, M.T.; Writing – Original Draft, M.T.; Writing – Review and Editing A.C.L., P.V., N.D., M.A.A., H.A., T.H., and M.G.; Visualization, M.A.A.; Supervision, M.G., and M.T.; Project Administration, T.H. and M.T.; Funding Acquisition, M.G., and M.T.

DECLARATION OF INTERESTS

The authors declare that the research was conducted without any commercial or financial relationships that could be construed as a potential conflict of interest.

REFERENCES

1. Moore, S.C., Lee, I.M., Weiderpass, E., Campbell, P.T., Sampson, J.N., Kitahara, C.M., Keadle, S.K., Arem, H., Berrington de Gonzalez, A., Hartge, P., et al. (2016). Association of Leisure-Time Physical Activity With Risk of 26 Types of Cancer in 1.44 Million Adults. JAMA Intern. Med. *176*, 816–825. https://doi.org/10.1001/jamainternmed.2016.1548.

2. Ashcraft, K.A., Peace, R.M., Betof, A.S., Dewhirst, M.W., and Jones, L.W. (2016). Efficacy and Mechanisms of Aerobic Exercise on Cancer Initiation, Progression, and Metastasis: A Critical Systematic Review of In Vivo Preclinical Data. Cancer Res. *76*, 4032–4050. https://doi.org/10.1158/0008-5472.CAN-16-0887.

3. Pedersen, L., Christensen, J.F., and Hojman, P. (2015). Effects of exercise on tumor physiology and metabolism. Cancer J. *21*, 111–116. https://doi.org/10.1097/PPO.0000000000000096.

4. Hojman, P., Gehl, J., Christensen, J.F., and Pedersen, B.K. (2018). Molecular Mechanisms Linking Exercise to Cancer Prevention and Treatment. Cell Metabol. *27*, 10–21. https://doi.org/10.1016/j.cmet.2017.09.015.

5. Morishita, S., Hamaue, Y., Fukushima, T., Tanaka, T., Fu, J.B., and Nakano, J. (2020). Effect of Exercise on Mortality and Recurrence in Patients With Cancer: A Systematic Review and Meta-Analysis. Integr. Cancer Ther. *19*, 1534735420917462. https://doi.org/10.1177/1534735420917462.

6. Alves, C.R.R., Neves, W.D., de Almeida, N.R., Eichelberger, E.J., Jannig, P.R., Voltarelli, V.A., Tobias, G.C., Bechara, L.R.G., de Paula Faria, D., Alves, M.J.N., et al. (2020). Exercise training reverses cancer-induced oxidative stress and decrease in muscle COPS2/TRIP15/ALIEN. Mol. Metabol. *39*, 101012. https://doi.org/10.1016/j.molmet.2020.101012.

7. Avancini, A., Belluomini, L., Tregnago, D., Trestini, I., Milella, M., Lanza, M., and Pilotto, S. (2021). Exercise and anemia in cancer patients: could it make the difference? Expert Rev. Hematol. *14*, 979–985. https://doi.org/10.1080/17474086.2021.2007764.

8. Marconcin, P., Marques, A., Ferrari, G., Gouveia, É.R., Peralta, M., and Ihle, A. (2022). Impact of Exercise Training on Depressive Symptoms in Cancer Patients: A Critical Analysis. Biology *11*, 614. https://doi.org/10.3390/biology11040614.

9. Hojman, P. (2017). Exercise protects from cancer through regulation of immune function and inflammation. Biochem. Soc. Trans. *45*, 905–911. https://doi.org/10.1042/BST20160466.

10. Koelwyn, G.J., Quail, D.F., Zhang, X., White, R.M., and Jones, L.W. (2017). Exercise-dependent regulation of the tumour microenvironment. Nat. Rev. Cancer *17*, 620–632. https://doi.org/10.1038/nrc.2017.78.

11. Rundqvist, H., Veliça, P., Barbieri, L., Gameiro, P.A., Bargiela, D., Gojkovic, M., Mijwel, S., Reitzner, S.M., Wulliman, D., Ahlstedt, E., et al. (2020). Cytotoxic T-cells mediate exercise-induced reductions in tumor growth. Elife *9*, e59996. https://doi.org/10.7554/eLife.59996.

12. Pedersen, L., Idorn, M., Olofsson, G.H., Lauenborg, B., Nookaew, I., Hansen, R.H., Johannesen, H.H., Becker, J.C., Pedersen, K.S., Dethlefsen, C., et al. (2016). Voluntary Running Suppresses Tumor Growth through Epinephrine- and IL-6-Dependent NK Cell Mobilization and Redistribution. Cell Metabol. *23*, 554–562. https://doi.org/10.1016/j.cmet.2016.01.011.

13. Pedersen, B.K. (2013). Muscle as a secretory organ. Compr. Physiol. *3*, 1337–1362. https://doi.org/10.1002/cphy.c120033.

14. Huang, Q., Wu, M., Wu, X., Zhang, Y., and Xia, Y. (2022). Muscle-to-tumor crosstalk: The effect of exercise-induced myokine on cancer progression. Biochim. Biophys. Acta, Rev. Cancer *1877*, 188761. https://doi.org/10.1016/j.bbcan.2022.188761.

15. Hashida, R., Matsuse, H., Kawaguchi, T., Yoshio, S., Bekki, M., Iwanaga, S., Sugimoto, T., Hara, K., Koya, S., Hirota, K., et al. (2021). Effects of a low-intensity resistance exercise program on serum miR-630, miR-5703, and Fractalkine/CX3CL1 expressions in subjects with No exercise habits: A preliminary study. Hepatol. Res. *51*, 823–833. https://doi.org/10.1111/hepr.13670.

16. Jee, H., Park, E., Hur, K., Kang, M., and Kim, Y. (2022). High-Intensity Aerobic Exercise Suppresses Cancer Growth by Regulating Skeletal Muscle-Derived Oncogenes and Tumor Suppressors. Front. Mol. Biosci. *9*, 818470. https://doi.org/10.3389/fmolb.2022.818470.

17. Catoire, M., Mensink, M., Kalkhoven, E., Schrauwen, P., and Kersten, S. (2014). Identification of human exercise-induced myokines using secretome analysis. Physiol. Genom. *46*, 256–267. https://doi.org/10.1152/physiolgenomics.00174.2013.

18. Della Gatta, P.A., Cameron-Smith, D., and Peake, J.M. (2014). Acute resistance exercise increases the expression of chemotactic factors within skeletal muscle. Eur. J. Appl. Physiol. *114*, 2157–2167. https://doi.org/10.1007/s00421-014-2936-4.

19. Pedersen, B.K., and Fischer, C.P. (2007). Beneficial health effects of exercise–the role of IL-6 as a myokine. Trends Pharmacol. Sci. *28*, 152–156. https://doi.org/10.1016/j.tips.2007.02.002.

20. Steensberg, A., van Hall, G., Osada, T., Sacchetti, M., Saltin, B., and Klarlund Pedersen, B. (2000). Production of interleukin-6 in contracting human skeletal muscles can account for the exercise-induced increase in plasma interleukin-6. J. Physiol. *529 Pt 1*, 237–242. https://doi.org/10.1111/j.1469-7793.2000.00237.x.

21. Fischer, C.P., Hiscock, N.J., Penkowa, M., Basu, S., Vessby, B., Kallner, A., Sjöberg, L.B., and Pedersen, B.K. (2004). Supplementation with vitamins C and E inhibits the release of interleukin-6 from contracting human skeletal muscle. J. Physiol. *558*, 633–645. https://doi.org/10.1113/jphysiol.2004.066779.

22. Ostrowski, K., Hermann, C., Bangash, A., Schjerling, P., Nielsen, J.N., and Pedersen, B.K. (1998). A trauma-like elevation of plasma cytokines in humans in response to treadmill running. J. Physiol. *513*, 889–894. https://doi.org/10.1111/j.1469-7793.1998.889ba.x.

23. Pedersen, B.K., and Febbraio, M.A. (2008). Muscle as an endocrine organ: focus on muscle-derived interleukin-6. Physiol. Rev. *88*, 1379–1406. https://doi.org/10.1152/physrev.90100.2007.

24. Gabriel, H., Urhausen, A., and Kindermann, W. (1992). Mobilization of circulating leucocyte and lymphocyte subpopulations during and after short, anaerobic exercise. Eur. J. Appl. Physiol. Occup. Physiol. *65*, 164–170. https://doi.org/10.1007/BF00705075.

25. Millard, A.L., Valli, P.V., Stussi, G., Mueller, N.J., Yung, G.P., and Seebach, J.D. (2013). Brief Exercise Increases Peripheral Blood NK Cell Counts without Immediate Functional Changes, but Impairs their Responses to ex vivo Stimulation. Front. Immunol. *4*, 125. https://doi.org/10.3389/fimmu.2013.00125.

26. Nielsen, H.B., Secher, N.H., Christensen, N.J., and Pedersen, B.K. (1996). Lymphocytes and NK cell activity during repeated bouts of maximal exercise. Am. J. Physiol. *271*, R222–R227. https://doi.org/10.1152/ajpregu.1996.271.1.R222.

27. Idorn, M., and Hojman, P. (2016). Exercise-Dependent Regulation of NK Cells in Cancer Protection. Trends Mol. Med. *22*, 565–577. https://doi.org/10.1016/j.molmed.2016.05.007.

28. Shephard, R.J. (2003). Adhesion molecules, catecholamines and leucocyte redistribution during and following exercise. Sports Med.

33, 261–284. https://doi.org/10.2165/00007256-200333040-00002.

29. Timmons, B.W., and Cieslak, T. (2008). Human natural killer cell subsets and acute exercise: a brief review. Exerc. Immunol. Rev. *14*, 8–23.

30. Bigley, A.B., Rezvani, K., Chew, C., Sekine, T., Pistillo, M., Crucian, B., Bollard, C.M., and Simpson, R.J. (2014). Acute exercise preferentially redeploys NK-cells with a highly-differentiated phenotype and augments cytotoxicity against lymphoma and multiple myeloma target cells. Brain Behav. Immun. *39*, 160–171. https://doi.org/10.1016/j.bbi.2013.10.030.

31. Bray, F., Ferlay, J., Soerjomataram, I., Siegel, R.L., Torre, L.A., and Jemal, A. (2018). Global cancer statistics 2018: GLOBOCAN estimates of incidence and mortality worldwide for 36 cancers in 185 countries. CA A Cancer J. Clin. *68*, 394–424. https://doi.org/10.3322/caac.21492.

32. Brenner, D.R., Yannitsos, D.H., Farris, M.S., Johansson, M., and Friedenreich, C.M. (2016). Leisure-time physical activity and lung cancer risk: A systematic review and meta-analysis. Lung Cancer *95*, 17–27. https://doi.org/10.1016/j.lungcan.2016.01.021.

33. Avancini, A., Sartori, G., Gkountakos, A., Casali, M., Trestini, I., Tregnago, D., Bria, E., Jones, L.W., Milella, M., Lanza, M., and Pilotto, S. (2020). Physical Activity and Exercise in Lung Cancer Care: Will Promises Be Fulfilled? Oncol. *25*, e555–e569. https://doi.org/10.1634/theoncologist.2019-0463.

34. Kurgan, N., Tsakiridis, E., Kouvelioti, R., Moore, J., Klentrou, P., and Tsiani, E. (2017). Inhibition of Human Lung Cancer Cell Proliferation and Survival by Post-Exercise Serum Is Associated with the Inhibition of Akt, mTOR, p70 S6K, and Erk1/2. Cancers *9*, 46. https://doi.org/10.3390/cancers9050046.

35. Paceli, R.B., Cal, R.N., dos Santos, C.H.F., Cordeiro, J.A., Neiva, C.M., Nagamine, K.K., and Cury, P.M. (2012). The influence of physical activity in the progression of experimental lung cancer in mice. Pathol. Res. Pract. *208*, 377–381. https://doi.org/10.1016/j.prp.2012.04.006.

36. Higgins, K.A., Park, D., Lee, G.Y., Curran, W.J., and Deng, X. (2014). Exercise-induced lung cancer regression: mechanistic findings from a mouse model. Cancer *120*, 3302–3310. https://doi.org/10.1002/cncr.28878.

37. Pedersen, K.S., Gatto, F., Zerahn, B., Nielsen, J., Pedersen, B.K., Hojman, P., and Gehl, J. (2020). Exercise-Mediated Lowering of Glutamine Availability Suppresses Tumor Growth and Attenuates Muscle Wasting. iScience *23*, 100978. https://doi.org/10.1016/j.isci.2020.100978.

38. Yan, L., and Demars, L.C. (2011). Effects of non-motorized voluntary running on experimental and spontaneous metastasis in mice. Anticancer Res. *31*, 3337–3344.

39. Miao, M., Masengere, H., Yu, G., and Shan, F. (2021). Reevaluation of NOD/SCID Mice as NK Cell-Deficient Models. BioMed Res. Int.

40. Stribbling, S.M., and Ryan, A.J. (2022). The cell-line-derived subcutaneous tumor model in preclinical cancer research. Nat. Protoc. *17*, 2108–2128. https://doi.org/10.1038/s41596-022-00709-3.

41. Häuselmann, I., Roblek, M., Protsyuk, D., Huck, V., Knopfova, L., Grässle, S., Bauer, A.T., Schneider, S.W., and Borsig, L. (2016). Monocyte Induction of E-Selectin-Mediated Endothelial Activation Releases VE-Cadherin Junctions to Promote Tumor Cell Extravasation in the Metastasis Cascade. Cancer Res. *76*, 5302–5312. https://doi.org/10.1158/0008-5472.CAN-16-0784.

42. Klintrup, K., Mäkinen, J.M., Kauppila, S., Väre, P.O., Mlkko, J., Tuominen, H., Tuppurainen, K., Mäkelä, J., Karttunen, T.J., and Mäkinen, M.J. (2005). Inflammation and prognosis in colorectal cancer. Eur. J. Cancer *41*, 2645–2654. https://doi.org/10.1016/j.ejca.2005.07.017.

43. Chiossone, L., Chaix, J., Fuseri, N., Roth, C., Vivier, E., and Walzer, T. (2009). Maturation of mouse NK cells is a 4-stage developmental program. Blood *113*, 5488–5496. https://doi.org/10.1182/blood-2008-10-187179.

44. Fu, B., Wang, F., Sun, R., Ling, B., Tian, Z., and Wei, H. (2011). CD11b and CD27 reflect distinct population and functional specialization in human natural killer cells. Immunology *133*, 350–359. https://doi.org/10.1111/j.1365-2567.2011.03446.x.

45. Meijer, J.H., and Robbers, Y. (2014). Wheel running in the wild. Proc. Biol. Sci. *281*, 20140210. https://doi.org/10.1098/rspb.2014.0210.

46. Manzanares, G., Brito-da-Silva, G., and Gandra, P.G. (2018). Voluntary wheel running: patterns and physiological effects in mice. Braz. J. Med. Biol. Res. *52*, e7830. https://doi.org/10.1590/1414-431X20187830.

47. Goh, J., Endicott, E., and Ladiges, W.C. (2014). Pre-tumor exercise decreases breast cancer in old mice in a distance-dependent manner. Am. J. Cancer Res. *4*, 378–384.

48. MacNeil, B., and Hoffman-Goetz, L. (1993). Exercise training and tumour metastasis in mice: influence of time of exercise onset. Anticancer Res. *13*, 2085–2088.

49. Goh, J., Tsai, J., Bammler, T.K., Farin, F.M., Endicott, E., and Ladiges, W.C. (2013). Exercise training in transgenic mice is associated with attenuation of early breast cancer growth in a dose-dependent manner. PLoS One *8*, e80123. https://doi.org/10.1371/journal.pone.0080123.

50. Welsch, M.A., Cohen, L.A., and Welsch, C.W. (1995). Inhibition of growth of human breast carcinoma xenografts by energy expenditure via voluntary exercise in athymic mice fed a high-fat diet. Nutr. Cancer *23*, 309–318. https://doi.org/10.1080/01635589509514385.

51. Kanarek, R.B., D'Anci, K.E., Jurdak, N., and Mathes, W.F. (2009). Running and addiction: precipitated withdrawal in a rat model of

activity-based anorexia. Behav. Neurosci. *123*, 905–912. https://doi.org/10.1037/a0015896.

52. Naghshvarian, M., Zarrindast, M.R., and Sajjadi, S.F. (2017). Voluntary Wheel Running Induces Exercise-Seeking Behavior in Male Rats: A Behavioral Study. Arch. Iran. Med. *20*, 740–745.

53. Haseman, J.K., Bourbina, J., and Eustis, S.L. (1994). Effect of individual housing and other experimental design factors on tumor incidence in B6C3F1 mice. Fund. Appl. Toxicol. *23*, 44–52. https://doi.org/10.1006/faat.1994.1077.

54. Palermo-Neto, J., Fonseca, E.S.M., Quinteiro-Filho, W.M., Correia, C.S.C., and Sakai, M. (2008). Effects of individual housing on behavior and resistance to Ehrlich tumor growth in mice. Physiol. Behav. *95*, 435–440. https://doi.org/10.1016/j.physbeh.2008.07.006.

55. Been, L.E., Gibbons, A.B., and Meisel, R.L. (2019). Towards a neurobiology of female aggression. Neuropharmacology *156*, 107451. https://doi.org/10.1016/j.neuropharm.2018.11.039.

56. Williamson, C.M., Lee, W., DeCasien, A.R., Lanham, A., Romeo, R.D., and Curley, J.P. (2019). Social hierarchy position in female mice is associated with plasma corticosterone levels and hypothalamic gene expression. Sci. Rep. *9*, 7324. https://doi.org/10.1038/s41598-019-43747-w.

57. Tsai, M.S., Kuo, M.L., Chang, C.C., and Wu, Y.T. (2013). The effects of exercise training on levels of vascular endothelial growth factor in tumor-bearing mice. Cancer Biomarkers *13*, 307–313. https://doi.org/10.3233/CBM-130359.

58. Keller, C., Steensberg, A., Pilegaard, H., Osada, T., Saltin, B., Pedersen, B.K., and Neufer, P.D. (2001). Transcriptional activation of the IL-6 gene in human contracting skeletal muscle: influence of muscle glycogen content. Faseb. J. *15*, 2748–2750. https://doi.org/10.1096/fj.01-0507fje.

59. Abbasi, A., de Paula Vieira, R., Bischof, F., Walter, M., Movassaghi, M., Berchtold, N.C., Niess, A.M., Cotman, C.W., and Northoff, H. (2016). Sex-specific variation in signaling pathways and gene expression patterns in human leukocytes in response to endotoxin and exercise. J. Neuroinflammation *13*, 289. https://doi.org/10.1186/s12974-016-0758-5.

60. Cortes, C.J., and De Miguel, Z. (2022). Precision Exercise Medicine: Sex Specific Differences in Immune and CNS Responses to Physical Activity. Brain Plast. *8*, 65–77. https://doi.org/10.3233/BPL-220139.

61. Morgado, J.P., Monteiro, C.P., Matias, C.N., Alves, F., Pessoa, P., Reis, J., Martins, F., Seixas, T., and Laires, M.J. (2014). Sex-based effects on immune changes induced by a maximal incremental exercise test in well-trained swimmers. J. Sports Sci. Med. *13*, 708–714.

62. Diakos, C.I., Charles, K.A., McMillan, D.C., and Clarke, S.J. (2014). Cancer-related

inflammation and treatment effectiveness. Lancet Oncol. 15, e493–e503. https://doi.org/10.1016/S1470-2045(14)70263-3.

63. Taniguchi, K., and Karin, M. (2014). IL-6 and related cytokines as the critical lynchpins between inflammation and cancer. Semin. Immunol. 26, 54–74. https://doi.org/10.1016/j.smim.2014.01.001.

64. Panagiotakos, D.B., Pitsavos, C., Chrysohoou, C., Kavouras, S., and Stefanadis, C.; ATTICA Study (2005). The associations between leisure-time physical activity and inflammatory and coagulation markers related to cardiovascular disease: the ATTICA Study. Prev. Med. 40, 432–437. https://doi.org/10.1016/j.ypmed.2004.07.010.

65. Bigley, A.B., and Simpson, R.J. (2015). NK cells and exercise: implications for cancer immunotherapy and survivorship. Discov. Med. 19, 433–445.

66. Fiuza-Luces, C., Valenzuela, P.L., Castillo-García, A., and Lucia, A. (2021). Exercise Benefits Meet Cancer Immunosurveillance: Implications for Immunotherapy. Trends Cancer 7, 91–93. https://doi.org/10.1016/j.trecan.2020.12.003.

67. Kurz, E., Hirsch, C.A., Dalton, T., Shadaloey, S.A., Khodadadi-Jamayran, A., Miller, G., Pareek, S., Rajaei, H., Mohindroo, C., Baydogan, S., et al. (2022). Exercise-induced engagement of the IL-15/IL-15Ralpha axis promotes anti-tumor immunity in pancreatic cancer. Cancer Cell 40, 720–737.e5. https://doi.org/10.1016/j.ccell.2022.05.006.

68. Gilreath, J.A., Stenehjem, D.D., and Rodgers, G.M. (2014). Diagnosis and treatment of cancer-related anemia. Am. J. Hematol. 89, 203–212. https://doi.org/10.1002/ajh.23628.

69. Furrer, R., Jauch, A.J., Nageswara Rao, T., Dilbaz, S., Rhein, P., Steurer, S.A., Recher, M., Skoda, R.C., and Handschin, C. (2021). Remodeling of metabolism and inflammation by exercise ameliorates tumor-associated anemia. Sci. Adv. 7, eabi4852. https://doi.org/10.1126/sciadv.abi4852.

70. Mori, K., Fujimoto-Ouchi, K., Onuma, E., Noguchi, M., Shimonaka, Y., Yasuno, H., and Nishimura, T. (2009). Novel models of cancer-related anemia in mice inoculated with IL-6-producing tumor cells. Biomed. Res. 30, 47–51. https://doi.org/10.2220/biomedres.30.47.

71. Noguchi-Sasaki, M., Sasaki, Y., Shimonaka, Y., Mori, K., and Fujimoto-Ouchi, K. (2016). Treatment with anti-IL-6 receptor antibody prevented increase in serum hepcidin levels and improved anemia in mice inoculated with IL-6-producing lung carcinoma cells. BMC Cancer 16, 270. https://doi.org/10.1186/s12885-016-2305-2.

72. Bregolat, N.F., Ruetten, M., Da Silva, M.C., Aboouf, M.A., Ademi, H., Büren, N.v., Armbruster, J., Stirn, M., Altamura, S., Marques, O., et al. (2022). Iron- and erythropoietin-resistant anemia in a spontaneous breast cancer mouse model. Haematologica 107, 2454–2465. https://doi.org/10.3324/haematol.2022.280732.

73. Langdon, J.M., Yates, S.C., Femnou, L.K., McCranor, B.J., Cheadle, C., Xue, Q.L., Vaulont, S., Civin, C.I., Walston, J.D., and Roy, C.N. (2014). Hepcidin-dependent and hepcidin-independent regulation of erythropoiesis in a mouse model of anemia of chronic inflammation. Am. J. Hematol. 89, 470–479. https://doi.org/10.1002/ajh.23670.

74. McCranor, B.J., Kim, M.J., Cruz, N.M., Xue, Q.L., Berger, A.E., Walston, J.D., Civin, C.I., and Roy, C.N. (2014). Interleukin-6 directly impairs the erythroid development of human TF-1 erythroleukemic cells. Blood Cells Mol. Dis. 52, 126–133. https://doi.org/10.1016/j.bcmd.2013.09.004.

75. Barra, N.G., Fan, I.Y., Gillen, J.B., Chew, M., Marcinko, K., Steinberg, G.R., Gibala, M.J., and Ashkar, A.A. (2017). High Intensity Interval Training Increases Natural Killer Cell Number and Function in Obese Breast Cancer-challenged Mice and Obese Women. J. Cancer Prev. 22, 260–266. https://doi.org/10.15430/JCP.2017.22.4.260.

76. Ahmadabadi, F., Saghebjoo, M., Hedayati, M., Hoshyar, R., and Huang, C.J. (2021). Treatment-induced tumor cell apoptosis following high-intensity interval training and saffron aqueous extract in mice with breast cancer. Phys. Int. https://doi.org/10.1556/2060.2021.00009.

77. Baldelli, G., De Santi, M., Gervasi, M., Annibalini, G., Sisti, D., Højman, P., Sestili, P., Stocchi, V., Barbieri, E., and Brandi, G. (2021). The effects of human sera conditioned by high-intensity exercise sessions and training on the tumorigenic potential of cancer cells. Clin. Transl. Oncol. 23, 22–34. https://doi.org/10.1007/s12094-020-02388-6.

78. Cao, L., Zhang, X., Ji, B., Ding, S., and Qi, Z. (2021). Moderate endurance training reduced hepatic tumourigenesis associated with lower lactate overload compared to high-intensity interval training. Clin. Exp. Pharmacol. Physiol. 48, 1239–1250. https://doi.org/10.1111/1440-1681.13536.

79. Zhang, X., Cao, L., Ji, B., Li, L., Qi, Z., and Ding, S. (2020). Endurance training but not high-intensity interval training reduces liver carcinogenesis in mice with hepatocellular carcinogen diethylnitrosamine. Exp. Gerontol. 133, 110853. https://doi.org/10.1016/j.exger.2020.110853.

80. Ge, Z., Wu, S., Qi, Z., and Ding, S. (2022). Compared with High-intensity Interval Exercise, Moderate Intensity Constant Load Exercise is more effective in curbing the Growth and Metastasis of Lung Cancer. J. Cancer 13, 1468–1479. https://doi.org/10.7150/jca.66245.

81. Ge, Z., Wu, S., Qi, Z., and Ding, S. (2022). Exercise modulates polarization of TAMs and expression of related immune checkpoints in mice with lung cancer. J. Cancer 13, 3297–3307. https://doi.org/10.7150/jca.76136.

82. Alves, C.R.R., das Neves, W., Tobias, G.C., de Almeida, N.R., Barreto, R.F., Melo, C.M., Carneiro, C.D.G., Garcez, A.T., Faria, D.D.P., Chammas, R., and Brum, P.C. (2018). High-intensity interval training slows down tumor progression in mice bearing Lewis lung carcinoma. JCSM Rapid Communications 1, 1–10. https://doi.org/10.1002/j.2617-1619.2018.tb00008.x.

83. Jones, L.W., Antonelli, J., Masko, E.M., Broadwater, G., Lascola, C.D., Fels, D., Dewhirst, M.W., Dyck, J.R.B., Nagendran, J., Flores, C.T., et al. (2012). Exercise modulation of the host-tumor interaction in an orthotopic model of murine prostate cancer. J. Appl. Physiol. (1985) 113, 263–272. https://doi.org/10.1152/japplphysiol.01575.2011.

84. Jones, L.W., Eves, N.D., Courneya, K.S., Chiu, B.K., Baracos, V.E., Hanson, J., Johnson, L., and Mackey, J.R. (2005). Effects of exercise training on antitumor efficacy of doxorubicin in MDA-MB-231 breast cancer xenografts. Clin. Cancer Res. 11, 6695–6698. https://doi.org/10.1158/1078-0432.CCR-05-0844.

85. Sáez, M.D.C., Barriga, C., García, J.J., Rodríguez, A.B., and Ortega, E. (2007). Exercise-induced stress enhances mammary tumor growth in rats: beneficial effect of the hormone melatonin. Mol. Cell. Biochem. 294, 19–24. https://doi.org/10.1007/s11010-005-9067-5.

86. Faustino-Rocha, A., Oliveira, P.A., Pinho-Oliveira, J., Teixeira-Guedes, C., Soares-Maia, R., da Costa, R.G., Colaço, B., Pires, M.J., Colaço, J., Ferreira, R., and Ginja, M. (2013). Estimation of rat mammary tumor volume using caliper and ultrasonography measurements. Lab Anim. 42, 217–224. https://doi.org/10.1038/laban.254.

87. Shu, J., Dolman, G.E., Duan, J., Qiu, G., and Ilyas, M. (2016). Statistical colour models: an automated digital image analysis method for quantification of histological biomarkers. Biomed. Eng. Online 15, 46. https://doi.org/10.1186/s12938-016-0161-6.

88. Thornton, B., and Basu, C. (2011). Real-time PCR (qPCR) primer design using free online software. Biochem. Mol. Biol. Educ. 39, 145–154. https://doi.org/10.1002/bmb.20461.

89. Livak, K.J., and Schmittgen, T.D. (2001). Analysis of relative gene expression data using real-time quantitative PCR and the 2(-Delta Delta C(T)) Method. Methods 25, 402–408. https://doi.org/10.1006/meth.2001.1262.

90. Pfaffl, M.W. (2001). A new mathematical model for relative quantification in real-time RT-PCR. Nucleic Acids Res. 29, e45. https://doi.org/10.1093/nar/29.9.e45.

STAR★METHODS

KEY RESOURCES TABLE

REAGENT or RESOURCE	SOURCE	IDENTIFIER
Antibodies		
Mouse monoclonal anti-mouse/human NK1.1	ThermoFisher, Switzerland	#MA1-70100 (RRID AB_2296673)
Rat polyclonal anti-mouse/human CD161c/NK1.1	BIOSS; US	#BS-4682R
Rabbit polyclonal anti-mouse/human HIF-2-alpha	Abcam, US	#ab199
Rabbit monoclonal [SP6] anti-mouse/rat/human Ki67	Abcam, US	#Ab16667
Rat monoclonal anti-mouse CD16/32 (Mouse BD Fc Block™)	BD Biosciences, Germany	#553142 (RRID AB_394656)
Rat monoclonal FITC anti-mouse CD3	BioLegend, US	#100203 (RRID AB_312660)
Rat monoclonal APC anti-mouse CD8	BioLegend, US	#100711 (RRID AB_312750)
Rat monoclonal Pacific Blue anti-mouse CD4	BioLegend, US	#100427 (RRID AB_493646)
Rat monoclonal PE/Cy7 anti-mouse CD19	BioLegend, US	#115519 (RRID AB_313654)
Mouse monoclonal APC/Cy7 anti-mouse NK-1.1	BioLegend, US	#108723 (RRID AB_830870)
Rat monoclonal Alexa Fluor700 anti-mouse/huamn CD11b	BioLegend, US	#101222 (RRID AB_493705)
Hamster monoclonal PE anti-mouse/rat/huamn CD27	BioLegend, US	#124209 (RRID AB_1236464)
Goat polyclonal Alexa647 anti-mouse	Invitrogen, Switzerland	#A21240 (RRID AB_2535809)
Goat polyclonal Biotin-SP (long spacer) AffiniPure anti-Rabbit	Jackson ImmunoResearch, US	#111-065-003 (RRID AB_2337959)
Critical commercial assays		
Avidin-biotin blocking kit	Vector Laboratories, US	#SP-2001
Vectastain ABC Kit	Vector Laboratories, US	#PK-4000
DAB	Agilent Dako, US	#K346889-2
U-PLEX Mouse IL-6 Assay	Meso Scale Discovery, US	#K152TXK-1
Zombie Yellow™ Fixable Viability Kit	BioLegend, US	#423103
ReliaPrep RNA Tissue Miniprep	Promega, Switzerland	#Z6110
RevertAid First Strand cDNA Synthesis Kit	ThermoFisher Scientific, Switzerland	#K1622
SYBR Green	ThermoFisher Scientific, Switzerland	#A25741
Corning® Matrigel® Growth Factor Reduced (GFR) Basement Membrane Matrix	Sigma Aldrich, Switzerland	CLS354230
Experimental models: Cell lines		
Murine LLC1 Lewis lung carcinoma cells	ATCC, US	CRL-1642™ (RRID:CVCL_4358)
Murine B16F10 melanoma cells	ATCC, US	CRL-6475™ (RRID:CVCL_0159)
Murine LLC1.1 Lewis lung carcinoma cells	Dr. Lubor Borsig, University of Zurich	N/A
Experimental models: Organisms/strains		
Male C57BL/6J mice	Charles River, Germany	N/A
Oligonucleotides		
qPCR primers	This paper	Table S2

(Continued on next page)

Continued

REAGENT or RESOURCE	SOURCE	IDENTIFIER
Software and algorithms		
GraphPad Prism	GraphPad Software , US	N/A
BD FACSDiva™	BD Biosciences, US	N/A
FlowJo V10.5	FlowJo, US	N/A
FIJI	National Institute of Health, US	N/A
Other		
Mouse running wheel	Columbus Instruments International, US	#0297-0521
Hall Effect Sensor with Mount	Columbus Instruments International, US	#0297-0501
Wheel Counter 8 Channel Interface with Software	Columbus Instruments International, US	#0297-0050
Quad CI-Bus [0272-4201] USB PC Interface with MDI Software	Columbus Instruments International, US	#0297-0051
ABL 800 Flex	Radiometer Medical ApS, Denmark	N/A
BD LSR II FortessaT M SORP	BD Bioscience, Germany	N/A
NanoZoomer 2.0-HT	Hamamatsu, Japan	N/A

RESOURCE AVAILABILITY

Lead contact

Further information and requests for resources and reagents should be directed to and will be fulfilled by the lead contact, Markus Thiersch (markus.thiersch@uzh.ch).

Materials availability

This study did not generate new unique reagents.

Data and code availability

- Data reported in this paper will be shared by the lead upon request.

- This study does not report original codes.

- Any additional information required to reanalyze the data reported in this paper is available from the lead contact upon request.

EXPERIMENTAL MODEL DETAILS

Cancer cell lines and cell culture

Murine Lewis lung carcinoma cells LLC1 (RRID:CVCL_4358) from ATCC and LLC1.1 lung cancer cells (kindly provided by Dr. Lubor Borsig, passaged once *in vivo* and isolated from an LLC1 lung metastasis[41]) were cultured in 10 cm culture dishes (Corning, USA) in low glucose Dulbecco's Modified Eagle Medium (DMEM) (ThermoFisher, Switzerland). Murine B16F10 melanoma cells (RRID:CVCL_0159) from ATCC were cultured in Roswell Park Memorial Institute Medium (RPMI, Gibco by Life Technologies). All media were supplemented with 10 % New-Born Calf Serum (NBCS) (ThermoFisher, Switzerland), 2 mM L-Glutamine (ThermoFisher, Switzerland), 20 mM HEPES buffer solution (ThermoFisher, Switzerland) and 1 % Penicillin/Streptomycin (ThermoFisher, Switzerland) at 37°C, room air with 5% CO_2 in Heracell 240 incubator (Heraeus #H240-CO_2). All cells were negative tested for mycoplasma infection.

Mice

Mouse experiments were performed following the ARRIVE guidelines, the Swiss animal law, and with the approval of the ethical committee of the respective local authorities (Kanton Zurich, ZH214/2017). Healthy male C57BL/6J mice (6-8 weeks old) were purchased from Charles River (Baden-Württemberg, Germany). All mice were kept at a 12 h light/12 h dark cycle (7 a.m. – 7 p.m. light phase) in a licensed animal facility of

the University of Zurich. The mice had free access to food (Kliba Nafag, Switzerland) and water in their cages. Bodyweight and habitus were recorded every other day.

METHOD DETAILS

Experimental design

All mice were kept in groups for 2-3 weeks in the animal facility to recover from transport before the start of the experiments. Then, 8-10 weeks-old mice were randomly allocated into a running and non-running control group. The sample size of running mice was limited by our running wheel setup, which allowed testing a maximum of 8 running mice in parallel. Therefore, we repeated most experiments multiple times. The exact sample size is indicated in the figure legends. Running mice were single-housed in cages with a running wheel (Columbus Instruments International, US, #0297-0521). Exercise starting shortly before or after tumor implantation may not be sufficient to suppress[83,84] or can even increase tumor growth.[2,85] Therefore, our mice (voluntarily) trained for 4-6 weeks with running wheels before cancer cell injection (Figure S4A). Non-running control mice were kept single-housed in cages with blocked running wheels. After the training phase, we injected tumor cells into running and non-running mice. Running and non-running mice were placed back into their cages with open or blocked running wheels until the end of the experiment. Wheel revolutions were recorded by a magnetic hall effect sensor (Columbus Instruments International, US, #0297-0501) connected to a Quad CI-Bus USB PC Interface (Columbus Instruments International, US, #0297-0051) and documented by MDI software in five-minute intervals. The running distance was calculated from wheel revolutions and running wheel dimensions (diameter 10.16 cm):

$$revolution \times wheel\ circumference\ (\pi \times wheel\ diameter) = running\ distance\ (cm)$$

The average daily running distance (km/day) indicates a time interval of 24 h, with mice running mainly in the dark phase. Running distances are shown in the result section and Table S1. To establish the orthotopic lung cancer and the B16F10 lung invasion model, mice were tail vein injected with 3.3×10^5 LLC1.1 lung cancer cells or 2×10^5 B16F10 melanoma cells in 100 μl Hanks' Balanced Salt Solution (HBSS) (ThermoFisher, Switzerland). For the subcutaneous LLC1 tumor model, isoflurane-anesthetized, shaved mice were injected with 5×10^5 LLC1 cells in 100 μl HBSS containing 20% matrigel (Corning, Sigma Aldrich, Switzerland) into the right flank. Tumor size was measured with a caliper, and tumor volume was calculated by the formula V=1/2 x Length x (Width)^2, with the length being the largest tumor diameter and the width the perpendicular tumor diameter.[86] Mice were euthanized with an overdose of pentobarbital (Esconarkon, Streuli Pharma, Switzerland) 21 days after cancer cell implantation or when humane endpoints (loss of body weight, tumor ulceration) were reached. Blood was retrieved from the right heart ventricle for hemoglobin and hematocrit measurements (ABL 800 Flex, Radiometer) and plasma isolation. Tissues were isolated and either snap-frozen and stored at -80°C, immediately used, or fixed in 4% paraformaldehyde (PFA) for 24 h for subsequent histological, immunofluorescent, or immunohistochemical analyses.

Histology and immunostainings

PFA-fixed tissues were paraffin-embedded, and 4 μm thick longitudinal tissue sections were cut. Sections were deparaffinated and either stained using hematoxylin-eosin or used for immunohistochemistry and immunofluorescence. We performed antigen retrieval by cooking tissue sections in 10 mM sodium citrate buffer with 0.05% Tween for 20 or 30 minutes for immunofluorescence staining of NK cells. After cooling down, tissue sections were blocked using normal goat serum (#G6767, Sigma Aldrich, Switzerland) and incubated overnight with an NK cell-specific antibody (1:100; #MA1-70100 NK1.1, ThermoFisher, Switzerland) followed by an incubation with Alexa647 labeled goat-anti-mouse antibody (1:200, #A21240, Invitrogen, Switzerland) for 60 min. DAPI was used to counterstain the tissue sections. For immunohistochemistry staining of NK cells, tissue sections were blocked 60 minutes using normal goat serum and an avidin-biotin blocking kit (#SP-2001, Vector Laboratories, US). Tissue sections were then incubated overnight with a 1:50 dilution of an NK cell-specific antibody (#BS-4682R, BIOSS, US) followed by incubation in a 1:500 dilution of a biotinylated goat-anti-rabbit antibody (#111-065-003, Jackson ImmunoResearch, US) for 60 min. Tissue sections were incubated in an ABC complex solution (Vectastain ABC Kit, #PK-4000, Vector Laboratories, US) followed by incubation in a Nickel-DAB staining solution (0.04% NiCl$_2$x6H$_2$O and 0.08% CoCl$_2$x6H$_2$O in 50 mM Tris-HCl buffer; pH7.6) with one drop of DAB (#K346889-2, Dako) per ml buffer. Immunohistochemistry of HIF-2α (#Ab199, Abcam, US) and Ki67 (#Ab16667, Abcam, US) (both in 1:100 dilution) was done similarly, except that we performed an antigen

retrieval before blocking as described above, and slides were stained without Nickel in a DAB-only solution. Slides were fully scanned (NanoZoomer 2.0-HT; Hamamatsu, Japan). To quantify the HIF-2α and Ki67 staining in lungs with tumor nodules, we used FIJI and the Immunohistochemistry (IHC) Image Analysis Toolbox plugin to isolate the brown DAB signal.[87] We determined the HIF-2α positive area and normalized it to the total lung or tumor nodule area. Ki67 counts were normalized against the total tumor nodule area.

Quantification of tumor nodules in lungs and immune cell infiltration scoring

Before paraffin embedding, the number of macroscopic tumor nodules on the dorsal and ventral surface of PFA-fixed lungs was manually counted by three blinded persons using a dissecting microscope, and the average count was calculated. Additionally, we analyzed the area of tumor nodules in the lung over the total lung area on hematoxylin-eosin-stained lung sections using FIJI. Immune cell infiltration at the edges of tumor nodules was analyzed by a four-degree scale.[42] Scans of hematoxylin-eosin-stained lung sections were analyzed for the presence of lymphoid cells, macrophages, and neutrophilic granulocytes using a scoring system from 0 to 3. A score of 0 indicated the absence of inflammation and immune cells; a score of 1 indicated few inflammatory cells without destruction of the tumor nodule tissue; a score of 2 indicated band-like infiltrate at the edges of tumor nodules with some destruction of the tumor nodule tissue due to inflammation; and a score of 3 indicated a severe inflammatory reaction, including cup-like zones at the edges of tumor nodules and noticeable tissue destruction. Four invading edges of each tumor nodule were systemically evaluated, and the average for each tissue section was calculated.

Plasma Il-6

Fresh whole blood containing heparin was centrifuged at 400 x g for 15 minutes to isolate plasma, which was processed immediately or snap-frozen and stored at -80°C until analysis. Plasma interleukin 6 (IL-6) was measured by ELISA using U-PLEX Mouse IL-6 Assay® (#K152TXK-1, Meso Scale Discovery, US).

Flow cytometry

Blood was centrifuged at 400 x g for 15 minutes. The blood pellet was repeatedly incubated in red blood cell lysis buffer (4.15 g NH_4Cl, 0.55 g $KHCO_3$, and 0.185 g EDTA disodium salt in 500 ml H_2O) centrifuged until a white pellet was obtained. After adjusting the samples to 1 million cells per 100 μl PBS, the Fc receptors of immune cells were blocked with 10 μg/ml unlabeled purified rat anti-mouse CD16/CD32 antibody (#553142, BD Biosciences, Germany). Dead cells were stained with the Zombie Yellow™ Fixable Viability Kit (#423103, BioLegend, US). After centrifuging at 400 x g for 3 min, cells were incubated with 100 μl of an antibody mix containing FITC anti-mouse CD3 (#100203, BioLegend, US), APC anti-mouse CD8a (#100711, BioLegend, US), Pacific Blue anti-mouse CD4 (#100427, BioLegend, US), PE/Cy7 anti-mouse CD19 (#115519, BioLegend, US), APC/Cy7 anti-mouse NK-1.1 (#108723, BioLegend, US), Alexa Fluor700 anti-mouse/human CD11b (#101222, BioLegend, US), and a PE anti-mouse/rat/human CD27 (#124209, BioLegend, US) antibody. Unstained samples were used to control for autofluorescence during the flow cytometry measurements. Cells were measured by flow cytometry (BD LSR II FortessaT M SORP, BD Bioscience, Germany). The data were acquired with the BD FACSDiva™ Software and analyzed with FlowJo V10.5. The gating strategy is described in Figure S4B.

RNA extraction and mRNA expression analyses

RNA was extracted from 10-20 mg of tissue using the ReliaPrep RNA Tissue Miniprep System (#Z6110, Promega, Switzerland). Muscle RNA was isolated using a modified protocol for fibrous tissue. First-strand cDNA was synthesized using RevertAid First Strand cDNA Synthesis Kit (#K1622, ThermoFisher Scientific, Switzerland). Samples (5 ng/μl cDNA) were analyzed by a SYBR Green (#A25741, ThermoFisher Scientific, Switzerland) semi-quantitative real-time PCR (qRT-PCR) (7500 Fast Real-Time PCR System, ThermoFisher Scientific, Switzerland). Primers for mRNA expression analyses were designed by primer 3[88] (Table S2). Before using primers for mRNA expression analyses, they were validated by qRT-PCR by i) melting curve analyses (mode integrated into the 7500 Fast Real-Time PCR System) and ii) on acrylamide gels to confirm the size and purity of PCR products. mRNA expression levels were calculated using the ΔΔCt method.[89,90]

QUANTIFICATION AND STATISTICAL ANALYSIS

We used GraphPad Prism for generating graphs and statistical analyzes. We used the student's t-test for normally distributed data and the Mann-Whitney test for nonparametrically distributed data. Data distribution was estimated with Shapiro-Wilk and Kolmogorov Smirnov test. For multiple comparisons, we used either the Kruskal Wallis test with Dunn's multiple comparison test for nonparametrically distributed data or a one-way ANOVA with the Bonferroni post hoc test. Correlations were tested by a Pearson or a Spearman correlation analysis. A p-value of 0.05 was considered statistically significant. Statistical details, including representation of data, dispersion, and precision measures, statistical analysis (including blinding), and sample size (n, number of replicates), are described in the figure legends.